January 2013

The Glucocorticoid-Induced Leucine Zipper And Immunomodulation In Extracorporeal Photochemotherapy

Jeffrey Scott Futterleib
Yale School of Medicine, jfutter23@gmail.com

The Glucocorticoid-Induced Leucine Zipper and Immunomodulation in Extracorporeal Photochemotherapy

A Thesis Submitted to the
Yale University School of Medicine
in Partial Fulfillment of the Requirements for the
Degree of Doctor of Medicine

by

Jeffrey Scott Futterleib

2013

Abstract

THE GLUCOCORTICOID-INDUCED LEUCINE ZIPPER AND IMMUNOMODULATION IN EXTRACORPOREAL PHOTOCHEMOTHERAPY.
Jeffrey S. Futterleib, Robert E. Tigelaar, Jaehyuk Choi, Richard L. Edelson.
Department of Dermatology, Yale University School of Medicine, New Haven, CT.

Extracorporeal photochemotherapy (ECP) induces antigen-specific immune tolerance in graft-*versus*-host disease and solid-organ transplant rejection, and involves the *ex vivo* exposure of peripheral blood mononuclear cells to 8-methoxypsoralen plus ultraviolet A light (PUVA). In this study, we developed an *in vitro* model of ECP to decipher the immunomodulatory mechanisms of PUVA. The glucocorticoid-induced leucine zipper (GILZ) is both necessary and sufficient for the generation of dexamethasone-induced tolerogenic dendritic cells (DCs). We hypothesized that PUVA-induced activation of GILZ may contribute to the immune tolerance observed after ECP therapy in graft-*versus*-host disease and solid-organ transplantation. We report that PUVA acts via two pathways culminating in GILZ up-regulation in human monocyte-derived dendritic cells (MoDCs). Firstly, PUVA directly induces GILZ expression in MoDCs in a dose-dependent fashion ($p < 0.01$). Secondly, PUVA acts indirectly through the generation of apoptotic lymphocytes to induce GILZ expression in an apoptotic cell dose-dependent fashion ($p < 0.01$). MoDCs treated with PUVA, and/or exposed to lymphocytes rendered apoptotic by PUVA, up-regulated GILZ, down-regulated CD80, CD86 and CD83, became resistant to LPS-induced maturation, increased IL-10 production, and decreased production of pro-inflammatory cytokines (IL-12, IFN-γ, IL-6, TNF-α), and chemokines (IL-8, MCP-1, MIP-1β, RANTES) (all $p < 0.05$). Knockdown of GILZ via transient transfection with GILZ siRNA, compared to scramble siRNA, reduced IL-10 production and increased IL-12 production, demonstrating that GILZ is necessary for generating this tolerogenic cytokine profile. This study uncovers a potential molecular explanation for the immunomodulatory effects of PUVA, specifically through the induction of GILZ and polarization of immature MoDCs into tolerogenic DCs, and has implications for better understanding how ECP induces antigen-specific immunosuppression *in vivo*.

Acknowledgements

I would first like to thank Dr. Richard Edelson and Dr. Robert Tigelaar for their wonderful mentorship and continued enthusiasm for this project. Without their encouragement and willingness to hear my ideas, none of this work would have been possible. Next, I would like to thank Dr. Jaehyuk Choi for offering new ideas and critically reviewing the data, and Dr. Michael Girardi, Eve Robinson, Renata Filler, Dr. Julia Lewis and David Khalil for their particularly helpful discussions. I would like to thank my thesis committee members, Dr. Mark Mamula and Dr. Mario Sznol, for taking the time to review this thesis and offer their suggestions. I would also like to thank the entire Department of Dermatology for their amazing support of medical students interested in careers in dermatology. Last, but not least, I would like to thank my family for their love and patience, and the value they placed on my education.

This work was supported by a Howard Hughes Medical Institute Research Training Fellowship grant, a grant from the New York Cardiac Foundation, the Yale Comprehensive Cancer Center grant 3P30CA16359-29, and the Yale Office of Student Research.

Table of Contents

Introduction

1.1. Ultraviolet Radiation

Ultraviolet (UV) radiation possesses potent immunosuppressive and anti-inflammatory properties that were only fully appreciated with the advent of molecular immunology (1). In 1974, Kripke first demonstrated that immunologic rejection of UV-induced murine skin tumors, transplanted into syngeneic mice, could be limited by irradiating the recipient animal with low-dose UV light (2). Moreover, tumor graft rejection could also be prevented by adoptively transferring T-lymphocytes from UV-irradiated mice into recipient animals (2). This finding suggested a systemic component to the immunosuppressive action of UV radiation, and ultimately led to the discovery of antigen-specific suppressor T-lymphocytes induced by UV radiation (3). Subsequently, UV radiation was shown to directly inhibit various antigen-presenting cells (APCs) of the skin (4), including Langerhans cells (5), demonstrating the capacity of UV radiation to modulate both the innate and adaptive immune response.

Given its higher energy content, UVB radiation (280-320 nm) acts directly on DNA, forming pyrimidine dimers, photo-products, and ultimately inducing programmed cell death (1). In contrast, UVA radiation (320-400 nm) is less energetic, and requires the use of photosensitizing agents to achieve similar cellular effects (1). In 1953, Lerner characterized a psoralen as the photoactive compound responsible for the photosensitizing properties of the *Ammi majus* plant (1). Approximately twenty years later, the combination of oral psoralens and UVA light was introduced for the treatment of psoriasis (6). Then in 1987, Edelson *et al.* developed extracorporeal photochemotherapy (ECP), a novel therapy derived from psoralens and UVA light, to

treat cutaneous T-cell lymphoma (CTCL) (7). Since its initial FDA approval for CTCL, ECP has also been shown to be an efficacious, glucocorticoid- and immunosuppressant-sparing treatment for a variety of diseases, including graft-*versus*-host disease (GVHD) (8), solid-organ allograft rejection (9), and autoimmune disease (10).

1.2. Extracorporeal Photochemotherapy

ECP consists of the *ex vivo* exposure of peripheral blood mononuclear cells (PBMC) to the photosensitizing agent 8-methoxypsoralen (8-MOP) and UVA light (now referred to as PUVA), followed by subsequent reinfusion into the patient (7). 8-MOP quickly penetrates cellular and nuclear membranes, and upon absorption of UVA light, forms DNA mono-adducts and intra-strand cross-links in a PUVA dose-dependent fashion (11). The resultant DNA damage blocks replication and transcription and culminates in a well-characterized pattern of lymphocyte apoptosis (12-14). An intrinsic apoptotic pathway is initiated within 20 minutes of exposure to PUVA, involving reactive oxygen species formation, damage to mitochondrial membranes, and capsase-3, -8, and -9 activation (15-17). Progressive lymphocyte apoptosis is observed over the course of 48 hr (16, 17), primarily mediated through an extrinsic apoptotic pathway involving FasL and Fas receptor (CD95) interactions (18).

Therapeutic doses of 8-MOP and UVA light were initially titrated for clinical use based on their ability to inhibit lymphocyte proliferation *in vitro* (19, 20), and doses generally range from 1 to 2 J/cm^2 of UVA light and 100 to 200 ng/mL of 8-MOP (6-8). At these therapeutic doses, approximately 50 to 60% of lymphocytes are rendered apoptotic 24 hr after PUVA treatment, and 70 to 90% have reached a stage of late

apoptosis by 48 hr (21). The effects of PUVA on APCs are more ambiguous, with some studies documenting a resistance (12, 21-23), and others a sensitivity (24-26), to apoptosis following PUVA treatment.

A persistent mystery surrounding ECP centers on how a single therapy can stimulate an immune response to target and eradicate malignant lymphocytes in patients with CTCL (27), while also suppress the immune response of auto-reactive lymphocytes in patients with GVHD, allograft rejection and autoimmune disease (28)? Although a unifying mechanism fully explaining ECP's clinical efficacy has not yet been described, modulation of dendritic cells (DCs) (24, 29, 30), induction of regulatory T-lymphocytes (Tregs) (24, 30, 31), lymphocyte apoptosis (12-14), and modulation of cytokine release (32, 33) have all been implicated.

1.3. Dendritic Cells

DCs are versatile APCs capable of eliciting robust immune responses to pathogenic and foreign antigens, while maintaining tolerance to benign and self-antigens (34-36). The decision to elicit a specific type of immune response depends on multiple factors, including the maturation state of the DC (37, 38), the profile of co-stimulatory molecule expression and cytokine secretion, the nature of the pathogenic stimulus, the antigen dose presented, and the milieu of the tissue microenvironment (34-38).

Classically, DCs mature after exposure to various danger and pro-inflammatory mediators, including danger-associated molecular patterns (DAMPs) and pathogen-associated molecular patterns (PAMPs) (34, 35). DAMPs and PAMPS are recognized by a variety of pattern recognition receptors, including Toll-like receptors (TLRs) (34, 35).

Mature DCs up-regulate antigen-presenting molecules, express high levels of co-stimulatory molecules, such as CD80 and CD86, and secrete pro-inflammatory cytokines, such as IL-12 (35). Mature DCs present peptides on major histocompatibility complex (MHC) class II molecules, and engage naïve T-lymphocytes through the T-cell receptor (TCR) (34, 35). Mature DCs effectively deliver the necessary second signals (e.g. CD80/CD86 through CD28), and third signals (e.g. IL-12, IFN-γ, Notch ligand) required for naïve T-lymphocytes to differentiate into effector T-lymphocyte subsets (e.g T_h1, T_h2, T_h17), thereby generating diverse immunogenic responses (34, 35). Maturation also regulates the life span of DCs through CD14-mediated nuclear factor of activated T-lymphocyte (NFAT) activation, leading to the initiation of DC apoptosis (39).

1.4. Tolerogenic Dendritic Cells

In contrast, tolerogenic DCs are semi-mature cells (37, 38), generally characterized by low expression of co-stimulatory molecules, active production of IL-10 and TGF-β, and reduced production of pro-inflammatory cytokines and chemokines (36, 40). Tolerogenic DCs are critical in promoting tissue homeostasis and maintaining peripheral tolerance to harmless foreign antigens, as well as to self-antigens (36, 41). Since their initial characterization, many agents have been investigated, with varying success rates, to promote the *in vitro* differentiation of tolerogenic DCs for therapeutic purposes in treating autoimmune diseases and allograft rejection (36, 40, 41). Growth factors, including the immunosuppressive cytokines IL-10 and TGF-β, vitamins A and D3, prostaglandin E_2, and retinoids have all been utilized (36, 40, 41). Various immunosuppressive drugs have also been studied, including glucocorticoids,

cyclosporine, and tacrolimus (36, 40, 41), and protocols for genetically modifying immature DCs using viral vectors have been developed (40).

Immune tolerance to self-antigens begins during development through mechanisms of central tolerance occurring primarily in the thymus (36). Through the process of central tolerance, DCs and medullary epithelial cells delete the majority of T-lymphocytes expressing TCRs with strong affinities for peptides derived from self-proteins (36, 42). In addition, some self-reactive naïve T-lymphocytes are thought to differentiate into Tregs, known as natural Tregs (42). Central tolerance mechanisms are overwhelmingly successful in preventing the vast majority of autoimmune disease (42). Nevertheless, some auto-reactive T-lymphocytes escape the thymus and enter peripheral tissues (42). Tissue damage and cellular necrosis, resulting from periods of inflammation and infection, release self-proteins that are not adequately represented in the thymus and which T-lymphocytes may potentially target in an auto-reactive fashion (41, 42). Peripheral tolerance mechanisms are then required to suppress immune responses to these exposed self-antigens, as well as to harmless foreign antigens, non-pathogenic commensal organisms in the lung and digestive tract, and antigens in immunologically privileged sites, such as the anterior chamber of the eye and testes (41).

To maintain peripheral tolerance to these antigens, tolerogenic DCs induce auto-reactive T-lymphocyte deletion and anergy, and also generate antigen-specific Tregs (36, 41, 42). Tolerogenic DCs present peptides on MHC-class II molecules, and in a similar manner as immunogenic DCs, engage naïve T-lymphocytes through the TCR (36, 41). However, TCR ligation and downstream signaling in the setting of limited, or absent, second signals (e.g. low CD80/CD86 to engage CD28) and third signals (e.g. low IL-12),

results in T-lymphocyte deletion or anergy (40-42). Deleting auto-reactive T-lymphocytes, or rendering them anergic and unable to respond to the presented antigen in future settings, enables tolerogenic DCs to establish peripheral tolerance to the presented antigens (41, 42). Furthermore, Tregs are critically important in maintaining peripheral tolerance, and generally are $CD4^{+}CD25^{+}$ T-lymphocytes expressing the Foxp3 transcription factor (43). Tolerogenic DCs present peptide in the context of active IL-10 and TGF-β secretion (42, 43), rendering them uniquely capable of generating antigen-specific Tregs both *in vitro* and *in vivo* (43, 44).

Multiple lines of evidence suggest that the induction of antigen-specific Tregs by tolerogenic DCs contributes to the therapeutic efficacy of ECP (24, 31). Firstly, *in vivo* murine models of ECP demonstrate that an infusion of ECP-treated donor cells significantly reduces established GVHD (45) and prolongs cardiac allograft survival (46, 47), through the generation of antigen-specific $CD4^{+}CD25^{+}Foxp3^{+}$ Tregs (45, 47). In the GVHD model, Gatza *et al.* report that in addition to increased numbers of $Foxp3^{+}$ Tregs derived from the donor's T-lymphocytes and bone marrow grafts, there was a corresponding decrease in the number of donor effector lymphocytes that had never been themselves exposed to PUVA (45). Thus, through both donor effector T-lymphocyte deletion and Treg formation, the donor's T-lymphocytes were rendered tolerant of foreign antigens within the recipient animal (45). In the cardiac allograft models, ECP-treated donor cells similarly delivered both donor alloantigen and regulatory signals to DCs of the transplant recipient (46, 47). The systemic anti-donor T- and B-lymphocyte responses were greatly decreased, in part through T-lymphocyte deletion and Treg induction, and tolerance to foreign antigens in the allogeneic graft was achieved (46, 47).

Secondly, ECP inhibits both the sensitization and effector phase of contact hypersensitivity, through the induction of Tregs and generation of IL-10, respectively (48). Thirdly, ECP was accompanied clinically by an increase in the percentage of circulating $CD4^+CD25^+Foxp3^+$ Tregs, from 8.9% to 29.1%, in ten patients with GVHD (49). Lastly, prolonged ECP has not been observed to increase the incidence of opportunistic infection or malignancy (24), and T-lymphocyte and B-lymphocyte responses to novel or recall antigens are conserved in ECP patients (50). Both of these observations suggest that antigen-specific effects, rather than global immunosuppression as seen with chronic glucocorticoid administration, are operating *in vivo* after ECP.

Classically, tolerogenic DCs were described as both phenotypically and functionally immature cells (36, 37). The original model by Steinman *et al.* stated that immature DCs present low levels of self-peptide in the context of low co-stimulatory molecule expression, and thereby mediate tolerance to self-antigens (34-36). This model was subsequently refined with the discovery of co-inhibitory molecules (37), including B7-H1 (programmed death ligand 1) and immunoglobulin-like transcript 3 (ILT-3), and with the realization that tolerogenic DCs actively secrete immunosuppressive molecules, including IL-10 and TGF-β (38). It is now evident that tolerogenic DCs are both phenotypically and functionally mature cells and perform specialized functions, analogous to immunogenic DCs (37, 38, 40). Thus, the paradigm of DC maturation as the critical switch between tolerance induction and immunity is no longer strictly valid. The term 'semi-mature,' has been coined to differentiate the unique phenotypic and functional characteristics of tolerogenic DCs from immunogenic DCs (37, 38).

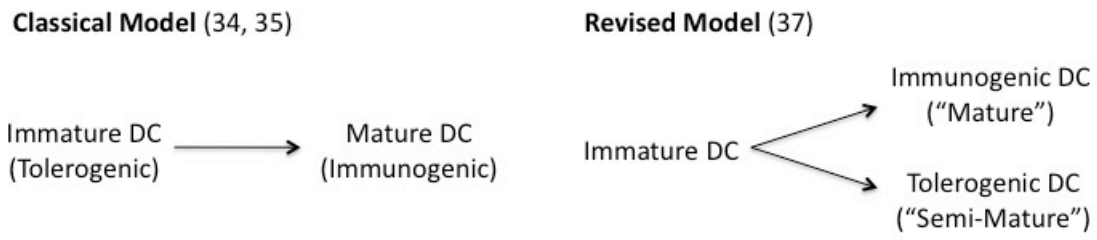

Apart from the questionable susceptibility of monocytes and DCs to apoptosis following ECP (12, 21-26), only a handful of studies have investigated the direct effects of ECP on monocyte and DC function. Studies examining the effects of ECP on these cell types have relied on procuring cells after treatment, or by irradiating cells *in vitro* using a UV light box. In one study, irradiated leukocytes from patients with chronic GVHD were isolated from the ECP bag after treatment (51). When these irradiated leukocytes were co-cultured with monocytes isolated before ECP from the same patient, production of both IL-10 and IL-1 receptor antagonist (IL-1Ra) were markedly increased (51, 52). Increased IL-10 production by monocytes was also observed following ECP in a separate analysis (23), along with reduced CD54, CD40 and CD86 co-stimulatory molecule expression (23). Likewise, an *in vitro* model of ECP designed by Legitimo *et al.* consisted of the co-culture of PUVA-treated monocytes with untreated monocytes in a nine to one ratio in an attempt to reproduce the extracorporeal exposure of approximately 10% of circulating monocytes to PUVA (53). In this model, the authors observed increased HLA-DR expression and endocytic capacity in the untreated monocytes, and a reduced ability to induce allogeneic T-lymphocyte proliferation (53).

Concerning the effects of ECP specifically on DC function, Spisek *et al.* analyzed myeloid DCs isolated from photopheretic products before reinfusion into patients with

refractory chronic GVHD (21). The authors reported significant production of IL-10, and virtually no IL-6 or IL-12 production by myeloid DCs after treatment (21). Another study also reported a decreased alloreactive capacity of DCs isolated after ECP (54), and a shift from a predominately T_h1 (IFN-γ) to T_h2 (IL-10 and IL-4) cytokine profile in patients with chronic GVHD (54). Finally, Berger *et al.* demonstrated that the ECP procedure itself induces monocyte-to-DC differentiation within a single day (29). The DCs produced during ECP were maturationally synchronized and functionally capable APCs (29), further suggesting that DCs play a central role in the therapeutic efficacy of ECP.

1.5. Glucocorticoid-Induced Leucine Zipper

Glucocorticoids have long been known to modulate APC function both *in vitro* and *in vivo* (55). Human DCs treated with dexamethasone increase mannose-receptor mediated endocytosis (56), reduce expression of the maturation molecule CD83 and the co-stimulatory molecule CD86 (55), increase production of IL-10 (57), and reduce production of IL-12 (57). Dexamethasone treatment also induces durable effects, with increases in IL-10, and decreases in IL-12, maintained for up to 5 days after removal of dexamethasone from DC cultures (58).

Until recently, the molecular signals driving an immature DC to be committed towards a tolerogenic phenotype and functional state were unknown. In 2006, Cohen *et al.* described an intracellular gene and protein product, highly expressed in human DCs after dexamethasone treatment, that was pivotal for the tolerogenic functions of DCs (59). The gene, called the glucocorticoid-induced leucine zipper (GILZ, also known as *TSC22*

domain family protein 3), was originally identified as a dexamethasone-responsive gene that protected murine T-lymphocytes from TCR/CD3-activated cell death (60). T-lymphocytes over-expressing GILZ demonstrated pronounced inhibition of TCR-activated nuclear factor κB (NF-κB), IL-2 production, FasL up-regulation, and ultimately activation-induced apoptosis (61). A variety of immunologic and non-immunologic cell types were subsequently discovered to also express GILZ, including macrophages (62), mast cells (63), bone marrow mesenchymal cells (64), and epithelial cells (65, 66). To date, GILZ has been implicated in an equally diverse number of cellular processes, including spermatogenesis (67), renal ion transport (65, 66), neuroendocrine functioning (68), and osteogenic differentiation (64).

In the original report by Cohen *et al.*, over-expression of GILZ by plasmid transfection, and silencing of GILZ with siRNA revealed that GILZ is both necessary and sufficient for the generation of tolerogenic human DCs (59). The expression of GILZ is also induced *in vivo* in patients receiving glucocorticoids (59). In a follow-up study by Hamdi *et al.*, human DCs expressing GILZ were found to be capable of inducing antigen-specific Tregs, and GILZ was necessary for this induction (69). The authors postulated that GILZ may be a molecular switch committing immature DCs towards the tolerogenic differentiation pathway (59, 69). According to this model, immature DCs do not express GILZ until exposed to immunosuppressive stimuli, such as glucocorticoids, IL-10, or TGF-β (59). Once GILZ is expressed at high levels, immature DCs differentiate into semi-mature tolerogenic DCs capable of generating Tregs and maintaining immune tolerance (59, 69). If immature DCs are instead exposed to traditional maturation stimuli, including inflammatory, microbial or danger signals, they do not express GILZ and

differentiate into mature immunogenic DC, capable of eliciting classical T_h1, T_h2, T_h17 or cytotoxic T-lymphocyte immune responses (34-36).

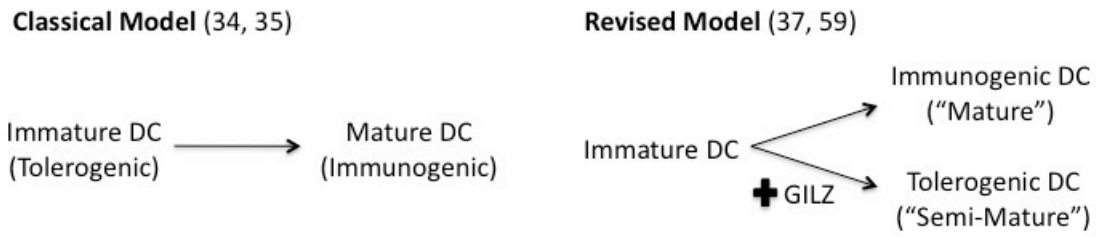

Human DCs expressing GILZ down-regulate co-stimulatory molecules and maturation markers (59, 70, 71), up-regulate molecules involved in maintaining peripheral tolerance, including PD-L1 and ILT-3 (70, 71), increase production of IL-10, reduce production of pro-inflammatory cytokines and chemokines, and are poor inducers of $CD4^+$ effector T-lymphocyte responses (59, 69-71). In addition, human DCs expressing GILZ generate IL-10 producing $CD4^+CD25^+Foxp3^+$ Tregs, capable of inhibiting $CD4^+$ and $CD8^+$ T-lymphocyte responses in an antigen-specific manner (69). In fact, the antigen-specific tolerance-inducing capacity of GILZ is exerted mainly through Treg induction (69-71).

In humans, GILZ codes for a cytosolic protein that directly binds to, and inhibits, a wide variety of signaling pathways that are highly active during inflammation, and in immunogenic DCs after ligation of TLRs, cytokine receptors, and chemokine receptors (70, 71). Specifically, GILZ binds to the p65 subunit of the prominent pro-inflammatory transcription factor NF-κB, preventing its nuclear translocation, DNA binding capacity, and transcriptional activity (72). GILZ also inhibits the mitogen activated protein kinase

(MAPK) family members Ras/Raf-1 (61, 67, 71), and ERK-1/2 (70, 71), and the activator protein 1 (AP-1) (70, 71). Given the importance of signal transduction pathways in integrating and amplifying cellular responses to pathogens and pro-inflammatory cytokines, the role of GILZ as a direct inhibitor of these pathways points towards its fundamental role as a regulator of the immune response (70, 71).

The expression of GILZ is induced to a lesser extent by both IL-10 and TGF-β (59). Like glucocorticoids (55-58), IL-10 blocks the maturation of DCs, reducing the expression of co-stimulatory molecules and the production of IL-12 (73), and TGF-β is critical for Treg induction (43). These observations suggest that GILZ may be a common molecular switch committing DCs towards a tolerogenic phenotype and functional state after exposure to diverse immunosuppressive stimuli (59, 69). While glucocorticoids bind to the glucocorticoid receptor, which transactivates the expression of glucocorticoid target genes including GILZ (70, 71), the molecular pathways linking IL-10 and TGF-β signaling to the induction of GILZ remain unknown.

1.6. Apoptotic Cells

The uptake of apoptotic cells by resident DCs not only maintains tissue homeostasis, but is also thought to induce peripheral tolerance through the presentation of self-antigens derived from apoptotic cells (41, 42). The ability of apoptotic cells to deliver immunosuppressive signals to APCs and reduce a pro-inflammatory response is also well documented (74-76). The extent of immunosuppression conferred by apoptotic cells depends on the nature of the apoptotic material (75, 76), the level of cellular destruction, ranging from early apoptosis to necrosis (77), and the route of apoptotic cell

administration (74, 75). Voll *et al.* first reported that monocytes, in the presence of apoptotic cells, increase production of IL-10 and decrease production of the pro-inflammatory cytokines TNF-α, IL-1β and IL-12 (74). Cell-contact was later demonstrated to be necessary for the induction of this immunosuppressive cytokine response (75). Moreover, monocytes cultured with ECP-treated apoptotic lymphocytes reduce production of the pro-inflammatory cytokines IL-1α (21, 32) and IL-6 (21, 32), and increase production of IL-10 (23, 52) and IL-1Ra (51, 52).

Similarly, apoptotic cells have been observed to modulate the functions of both macrophages (78) and DCs (77-79). Immature DCs are capable of recognizing and internalizing PUVA-treated cells undergoing apoptosis (31, 45-47). After internalizing apoptotic cells, DCs acquire a tolerogenic phenotype (53, 80, 81), down-regulate expression of co-stimulatory molecules (80, 81), increase production of IL-10 (48, 79, 81), and become poor stimulators of naïve T-lymphocytes (79-81). The downstream molecular pathways contributing to the induction of tolerogenic DCs by apoptotic cells remain unclear, however receptors involved in the recognition and uptake of apoptotic bodies are likely involved (74).

The exposure of phosphatidylserine on the outer leaflet of the plasma membrane and loss of membrane phospholipid asymmetry is one of the earliest cellular events occurring during apoptosis (82, 83). Phosphatidylserine is recognized by TAM (Tyro3, Axl and Mer) receptors on the surface of DCs (84), and through a combination of the thrombospondin receptor (CD36) (78) and other scavenger receptors, including the vitronectine ($\alpha_V\beta_3$ integrin) receptor (74), DCs recognize and internalize apoptotic cells. Phosphatidylserine and CD36 have particularly important roles in delivering

immunosuppressive signals, as evidenced by the ability to mimic the inhibitory effects of apoptotic cells with only phosphatidylserine-containing liposomes (85) or anti-CD36 (83).

In summary, ECP induces antigen-specific immunosuppression in GVHD (45) and solid-organ transplant rejection (46, 47), and this immunomodulation is largely mediated through the generation of antigen-specific Tregs (45-48). Moreover, both UV radiation (1, 2) and apoptotic cells (74, 77-79) transmit immunosuppressive signals to DCs, and the phenotypic and functional characteristics of tolerogenic DCs are essential for inducing Tregs differentiation from naïve T-lymphocytes (41-43). Given this set of observations, combined with the central role of GILZ in generating tolerogenic DCs (59) and Tregs (69), we hypothesized that PUVA directly induces GILZ expression in immature DCs, thereby polarizing them towards a tolerogenic phenotype and functional state. We further hypothesized that the immunosuppressive signals delivered by lymphocytes, rendered apoptotic by PUVA, induce GILZ expression in a similar fashion as glucocorticoids, IL-10 and TGF-β. We developed a co-culture of human monocyte-derived DCs (MoDCs) and apoptotic lymphocytes (ApoL) as an *in vitro* model of ECP to help decipher the direct and indirect immunosuppressive effects of PUVA.

Hypotheses

Hypothesis A*:* PUVA directly induces GILZ expression in immature MoDCs in a dose-dependent fashion and polarizes MoDCs towards a tolerogenic phenotype and function.

Hypothesis B**:** PUVA indirectly induces GILZ expression through the generation of ApoL that are subsequently recognized by immature MoDCs. ApoL induce GILZ expression in immature MoDCs, polarizing them towards a tolerogenic phenotype and function.

Specific Aims

Specific Aim 1*:* To differentiate human monocytes into immature MoDCs in the presence of GM-CSF and IL-4, and determine the dexamethasone dose-dependent induction of GILZ to serve as a positive control.

Specific Aim 2*:* To quantify the susceptibilities of immature MoDCs and lymphocytes to the apoptotic effects of PUVA.

Specific Aim 3: To determine if PUVA treatment and apoptotic cell exposure induces GILZ expression in immature MoDCs.

Specific Aim 4**:** To characterize the phenotypic profile of MoDCs expressing GILZ at high levels after PUVA treatment and/or apoptotic cell exposure, including expression of the maturation marker CD83, and the co-stimulatory molecules CD80 and CD86.

Specific Aim 5**:** To characterize the functional profile of MoDCs expressing GILZ at high levels after PUVA treatment and/or apoptotic cell exposure, including production of IL-10 and various pro-inflammatory cytokines and chemokines, including IL-12.

Specific Aim 6**:** To establish if GILZ induction is responsible for the tolerogenic cytokine profile observed after PUVA treatment and/or apoptotic cell exposure, specifically in regards to the IL-10 to IL-12 ratio.

Methods

3.1. Authorship

JSF formulated the hypotheses regarding the induction of GILZ after exposure of MoDCs to PUVA and apoptotic cells. JSF, in collaboration with RLE, RET and JC, designed all experiments to provide laboratory support for these postulates. JSF performed all of the methods, procedures and experiments described below. JSF, along with RLE, RET and JC, analyzed and interpreted the data.

3.2. Sample Collection

Whole blood was acquired from healthy subjects under the guidelines of the Yale Human Investigational Review Board, and informed consent was provided according to the Declaration of Helsinki. Peripheral blood specimens were obtained by standard venipuncture into syringes containing 0.1% heparin, and PBMC were isolated by centrifugation over a Ficoll-Hypaque gradient (Isolymph, CTL Scientific, Deer Park, NY). Cell viability was assessed by Trypan blue exclusion and PBMC were utilized immediately after isolation.

3.3. Monocyte Enrichment

Freshly isolated PBMC were plated in 6-well polystyrene tissue culture plates at a concentration of 5 x 10^6 cells/mL in RPMI-1640 (Gibco, Carlsbad, CA) supplemented with 15% heat-inactivated human AB serum (Gemini, Sacramento, CA), L-glutamine, and 25 mM HEPES. Monocytes were allowed to adhere to the plastic culture plate for 2 hr at 37^{o}C and 5% CO_2, after which non-adherent cells were removed, and adherent cells

were vigorously washed with RPMI-1640 and incubated for an additional 1.5 hr at 37°C and 5% CO_2. Non-adherent cells were once again removed, and adherent cells were vigorously washed as previously described. The purity of adherent and non-adherent cells was determined by CD14 and CD3 flow cytometric staining (purity: 71.6 ± 5.6% $CD14^+$). Non-adherent cells (purity: 66.0 ± 4.5% $CD3^+$) removed during plastic adherence will now be referred to as lymphocytes.

Monocytes were also enriched from freshly isolated PBMC by negative selection using the Monocyte Isolation Kit II (Miltenyi Biotec, Auburn, CA) according to the manufacturer's instructions, with the following modification: The purification buffer was optimized to PBS supplemented with 2% autologous serum and 1 mM EDTA. Isolation of unlabeled monocytes was achieved by negatively depleting the magnetically labeled cells incubated with an antibody cocktail consisting of anti-human CD3, CD7, CD16, CD19, CD56, CD123 and glycophorin A. The purity of enriched cells was determined by CD14 flow cytometric staining (purity: 83.8 ± 3.8% $CD14^+$).

Finally, monocytes were enriched from freshly isolated PBMC by CD14 positive magnetic bead selection according to the manufacturer's instructions (Miltenyi Biotec, Auburn, CA), with the following modifications: 1.) The purification buffer was optimized to PBS supplemented with 0.5% AB serum and 2 mM EDTA; 2.) 20 µL FcR blocker (Miltenyi Biotec, Auburn, CA) was added to 10^7 cells and incubated for 10 min on ice; 3.) 2 µL anti-human CD14 -biotin labeled antibody (clone 61D3, eBioscience, San Diego, CA) was then added to 10^7 cells and incubated for 20 min on ice; 4.) After washing with purification buffer, 20 µL anti-biotin microbeads (Miltenyi Biotec, Auburn, CA) were added to 10^7 cells and incubated for 15 min on ice. Cells were passed over a MACS

separator column in a magnetic field (Miltenyi Biotec, Auburn, CA). Magnetically labeled $CD14^+$ monocytes were retained in the column, and the unlabeled cells were washed off and saved. After removal of the column from the magnetic field, magnetically labeled $CD14^+$ monocytes were eluted as a positively selected fraction. The purity of enriched cells was determined by CD14 flow cytometric staining (purity: 88.1 ± 3.5% $CD14^+$).

3.4. Generation of Immature Monocyte-Derived DCs

Enriched monocytes were cultured at a density of 5 x 10^6 cells/mL in 6- and 12-well polystyrene tissue culture plates at 37°C and 5% CO_2 in RPMI-1640 supplemented with heat-inactivated 15% human AB serum and 1% penicillin/streptomycin (now referred to as complete media). 800 IU/mL recombinant human GM-CSF (R&D Systems, Minneapolis, MN) and 1000 IU/mL recombinant human IL-4 (R&D Systems, Minneapolis, MN) were added to cultures for 36 hr to induce monocyte to immature DC differentiation as described (86). In comparative studies, MoDCs generated in 48 hr are comparable with traditional MoDCs (87, 88) cultured for 5 days both phenotypically and functionally (88, 89), and equally capable of eliciting T-lymphocyte responses *in vitro* (86). After 36 hr, the immunophenotype of cells was analyzed to ensure that they possessed an immature MoDC phenotype.

3.5. 8-MOP and UVA Light Treatment

Cultures were incubated with 20 μg/mL 8-MOP (Therakos, Raritan, NJ) for 30 min in the dark, and then irradiated with a desktop UVA light box containing a series of

12 linear fluorescent tubes. Cells were washed once with PBS after treatment, and replaced with fresh complete media. The tubes emitted UVA light ranging from 320 to 400 nm, with a peak emission of 365 nm. The UVA irradiance (power, W/m^2) was measured using a photodiode, removing visible light (>400 nm) with a low-pass filter. The radiation emission of the lamp and the transmission characteristics of the media and plastic plates used for cell culture were evaluated in order to determine their absorption properties. Given a measured irradiance emitted from the fluorescent tubes, and the absorption properties of the various components of the system, it was possible to determine the time (sec) needed to expose the cells to deliver a given dose of UVA radiation (J/cm^2). A direct comparison between RPMI-1640 with or without phenol red revealed no difference in the kinetics of lymphocyte apoptosis, and RPMI-1640 with phenol red was chosen for all experiments involving 8-MOP and UVA light.

3.6. MoDC/Lymphocyte Co-Cultures

Cultures of MoDCs and lymphocytes were treated with PUVA independently. Lymphocytes were treated with 8-MOP (100 ng/mL) and UVA light (1 J/cm^2), washed once with PBS, counted, and co-cultured with either PUVA-treated or untreated MoDCs in a ratio of five or ten lymphocytes to one MoDC. PUVA-treated and untreated MoDCs were also cultured alone, with no lymphocytes added. MoDCs treated for 24 hr with 100 nM dexamethasone (Sigma, Ronkonkoma, NY) were chosen as the positive control group (59). All cells were cultured at 37°C and 5% CO_2 in complete media. After 24 hr, cells from all groups were harvested and MoDCs were re-purified. Given that lymphocytes also express GILZ (60), it was critical to re-purify MoDCs from all cultures to ensure that

RNA was not isolated in significant quantity from lymphocytes. MoDCs were re-purified using CD11c magnetic bead positive selection (purity: 96.4 ± 1.0% $CD11c^+$, 3.2 ± 1.1% $CD3^+$ cell contamination) according to the manufacturer's instructions (Miltenyi Biotec, Auburn, CA). The CD11c positive magnetic bead selection was performed in an identical fashion as previously described for the CD14 positive magnetic bead selection of monocytes. $CD11c^+$ MoDCs were then re-plated at 0.5 to 1.0 x 10^6 cells/mL in complete media and stimulated with 100 ng/mL lipopolysaccharide (LPS, from *E. coli* 026:B6) (Sigma, Ronkonkoma, NY). 24 hr after LPS stimulation, cells were harvested for RNA isolation and flow cytometric analysis, and supernatants were collected for cytokine quantification. Parallel groups not receiving LPS were also analyzed.

3.7. siRNA-Mediated GILZ Knockdown

Silencer select pre-designed (inventoried) and validated GILZ siRNA (Invitrogen, Carlsbad, CA; TSC22D3, sense: GCUUUGGGAUGACCGCUUAtt, antisense: UAAGCGGUCAUCCCAAAGCtg), with off-target prediction algorithms, was used to transiently knockdown GILZ expression in MoDCs. MoDCs were transfected using the Lipofectamine RNAiMAX Reagent according to the manufacturer's instructions (Invitrogen, Carlsbad, CA). Opti-MEM I Reduced Serum Medium (Invitrogen, Carlsbad, CA) was used to incubate diluted RNA_i duplex and lipofectamine reagent for 20 min at room temperature. RNA_i duplex-lipofectamine complexes were then added to MoDC cultures and incubated for 2 hr at 37°C and 5% CO_2. Transfected MoDCs were treated in an identical fashion as described for the MoDC/lymphocyte co-cultures. MoDCs were

also transfected with scramble siRNA as a control. Each group contained a culture that was not transfected. Transfection efficacy was determined by qRT-PCR.

3.8. Immunophenotyping

Monoclonal antibodies specific for monocytes and DCs included: HLA-DR FITC (Beckman Coulter, Brea, CA; clone Immu-357), CD80 FITC (Beckman Coulter, Brea, CA; clone MAB104), CD83 PE (Biolegend, San Diego, CA; clone HB15e), CD3 PE (Biolegend, San Diego, CA; clone OKT3), CD86 PE (Biolegend, San Diego, CA; clone IT2.2), GILZ PE (eBioscience, San Diego, CA; clone CFMKG15), CD14 PerCP/cy5.5 (eBioscience, San Diego, CA; clone 61D3), and CD11c APC (Biolegend, San Diego, CA; clone 3.9). Antibodies were used at their pre-determined optimal dilutions and staining was performed in the dark in FACS buffer (PBS plus 1% AB serum).

Apoptosis was assessed using the Annexin-V Apoptosis Detection Kit (eBioscience, San Diego, CA), according to the manufacturer's instructions, with 7-AAD substituting for PI as the cell viability dye. Annexin-V binds phosphatidylserine on the surface of apoptotic cells as the cell loses the ability to maintain membrane phospholipid asymmetry (82). Phosphatidylserine exposure is the one of the earliest events that occurs once a cell begins the process of apoptosis (82, 83). 7-AAD has a strong affinity for nuclear DNA, and is an indicator of cell membrane integrity. When a cell is in a late stage of apoptosis, or is undergoing secondary necrosis, the integrity of the cell membrane may become compromised, and the cell's DNA will stain with 7-AAD. Cells displaying an Annexin-V^+/7-AAD^- phenotype were classified as early apoptotic cells, and cells displaying an Annexin-V^+/7-AAD^+ phenotype were classified as late apoptotic cells.

Dual membrane and intra-cytoplasmic staining was performed using the IntraPrep fix and permeabilization kit (Beckman-Coulter, Brea, CA), according to the manufacturer's instructions. Intracytoplasmic staining was performed with GILZ and CD83. Background staining was established with appropriate isotype and fluorescence minus one controls. Immunofluorescence was analyzed using a FACSCalibur L (BD Biosciences, San Jose, CA) within 2 hr of fixation with 2% paraformaldehyde. A minimum of 10,000 events were collected for each group. Raw data was analyzed using FlowJo software (TreeStar, Can Carlos, CA).

3.9. Quantitative Real-Time PCR

RNA was isolated from $CD11c^+$ MoDCs using QIAShredder columns (QIAGEN, Hilden, Germany) and the RNeasy Mini Kit (QIAGEN, Hilden, Germany), with on-column Dnase I treatment (QIAGEN, Hilden, Germany), according to the manufacturer's instructions. RNA yield and purity were assessed using a NanoDrop ND-1000 spectrophotometer (NanoDrop Technologies, Wilmington, DE). The A260/280 ratio of isolated RNA was consistently between 1.8 and 2.1, with RNA yields ranging from 100 ng to 5 µg. Up to 1 µg of RNA was immediately reverse transcribed to cDNA using the High Capacity cDNA Reverse Transcription Kit (Applied Biosystems, Middletown, CT) according to the manufacturer's instructions. Reverse transcription was performed in a 96-well thermocycler (MJ Research PTC-200, Waltham, MA), with the following run conditions: 25° C (10 minutes), 37° C (120 minutes), 85° C (5 seconds). TaqMan real-time PCR was used to detect transcripts of GILZ, HPRT-1, CD80, and CD86. Primers and probes were obtained as pre-designed and validated Taqman Gene Expression

Assays (Applied Biosystems, Middletown, CT). SYBR green real-time PCR with Power SYBR Green Master Mix (Applied Biosystems, Middletown, CT) was used to detect transcripts of IL-12, IL-10, IL-6, TNF-α, TGF-β and GAPDH. Primers were designed to span intron junctions using Primer3Plus and the CCDS consensus sequence for each gene. Primer melting curves were obtained to confirm a single product and exclude primer-dimer formation. HPRT-1 and GAPDH were used as reference genes. Samples were run in triplicate on a 7500 Real Time PCR System (Applied Biosystems, Middletown, CT), and raw data was analyzed using 7500 Software v.2.0.5. The delta-delta C(t) method was used to calculate the fold change relative to control cells. Primer sequences are listed below for each gene.

IL-6 - $Primer_F$: GAGCTGTGCAGATGAGTACAAAA; $Primer_R$: GCATTTGTGGTTGGGTCAG

IL-10 - $Primer_F$: TCCCTGTGAAAACAAGAGCA; $Primer_R$: TGTCAAACTCACTCATGGCTTT

IL-12a - $Primer_F$: CAAGACCATGAATGCAAAGC; $Primer_R$: TCAAGGGAGGATTTTTGTGG

IL-12b - $Primer_F$: TGACATTCTGCGTTCAGGTC; $Primer_R$: CATTTTTGCGGCAGATGAC

TNF-α - $Primer_F$: GACAAGCCTGTAGCCCATGT; $Primer_R$: GAGGTACAGGCCCTCTGATG

TGF-β - $Primer_F$: GGCTTCTTGGTGCTGATGTC; $Primer_R$: TGCTTGGCAAACTCAGTGTC

GAPDH - $Primer_F$: CAATGACCCCTTCATTGACC; $Primer_R$: GACAAGCTTCCCGTTCTCAG

3.10. Cytokine Quantification

Culture supernatants were collected 24 hr after LPS stimulation, centrifuged at 1700 rpm for 10 min at 4°C to remove cells and debris, and immediately frozen at -80° C for future cytokine and chemokine quantification. Supernatants were thawed on ice and cytokine and chemokines were analyzed in a multiplex format utilizing magnetic beads to

IL-6, IL-8, IL-10, IL-12p70, IFN-γ, TNF-α, RANTES, MCP-1, and MIP-1β (BioRad Laboratories, Hercules, CA). For siRNA experiments, supernatants were analyzed with enzyme-linked immunosorbent assay (ELISA) kits for IL-10 (R&D Systems, Minneapolis, MD) and IL-12p70 (Enzo Life Science, Farmingdale, NY). All samples and standards were run in duplicate and analyzed using the LUMINEX 200 (LUMINEX, Austin TX), or the BioTek EL800 (BioTek, Winooski, VT).

3.11. Statistical Analysis

Student's *t*-tests (paired and unpaired) were used for statistical comparisons between groups, with p-values < 0.05 considered statistically significant. Differential gene expression was considered statistically significant with a ≥ 2.5-fold change and a p-value < 0.05.

Results

4.1. Figure 1

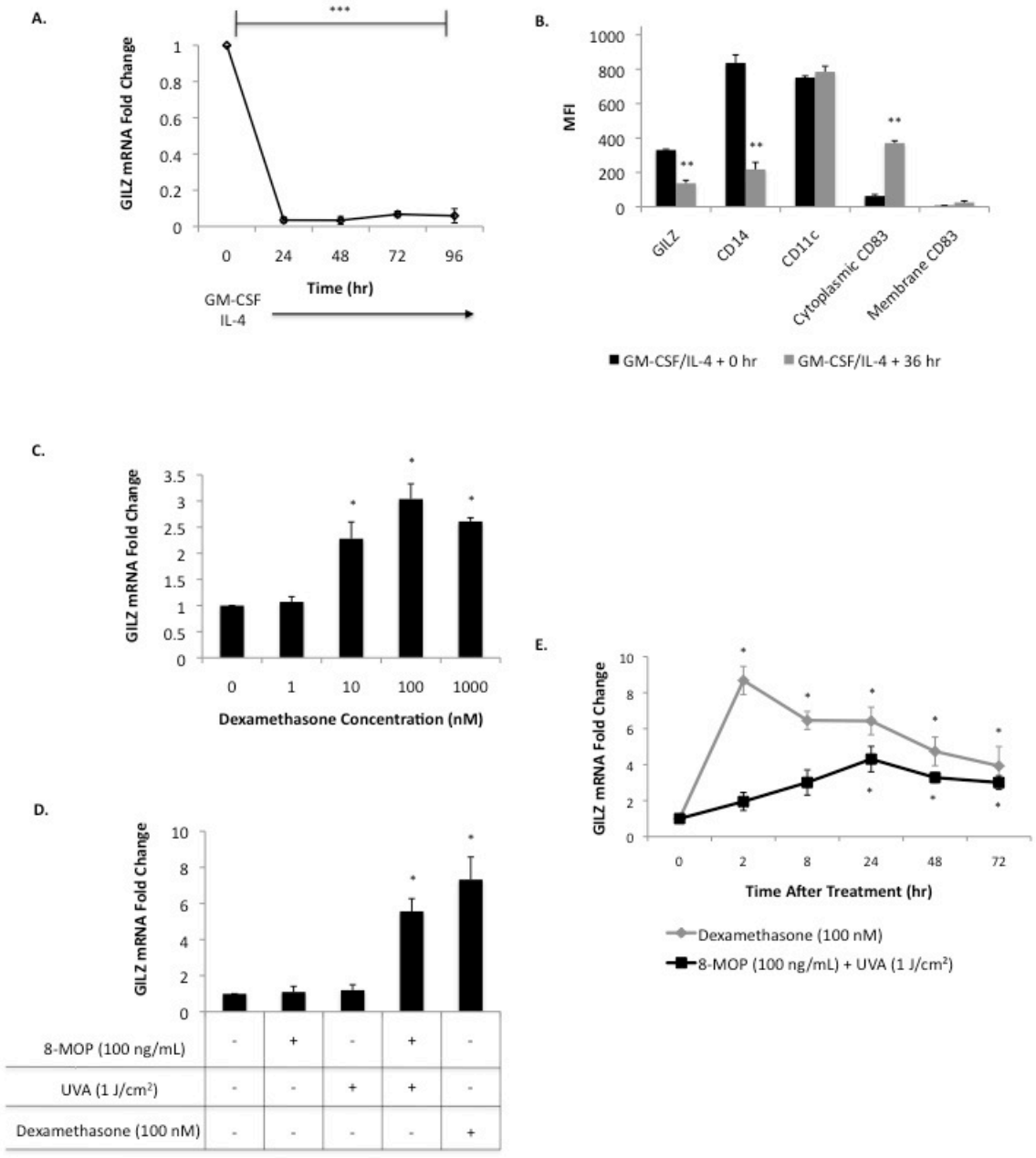

Figure 1: GILZ expression was rapidly down-regulated as monocytes differentiated into immature MoDCs, and up-regulated after exposure to dexamethasone. Total RNA was isolated from MoDCs. **A.)** GILZ mRNA expression in $CD11c^{+}$ MoDCs is presented as a fold change relative to freshly isolated monocytes. **B.)** Median fluorescence intensities for intracellular markers (GILZ, CD83) and cell surface markers (CD11c, CD14, CD83) in $CD11c^{+}$-gated MoDCs after 36 hr of culture with GM-CSF and

IL-4. **C.)** GILZ mRNA expression in $CD11c^+$ MoDCs after 24 hr is presented as a fold change relative to MoDCs receiving no dexamethasone. **D.)** GILZ mRNA expression in $CD11c^+$ MoDCs after 24 hr is presented as a fold change relative to untreated MoDCs. **E.)** GILZ mRNA expression in $CD11c^+$ MoDCs is presented as a fold change relative to untreated MoDCs. All data are expressed as mean ± standard deviation for a minimum of 3 independent experiments. For differential gene expression, a ≥ 2.5-fold change was chosen as the lower limit for considering statistically significant gene induction. $*p < 0.05$, $**p < 0.01$, $***p < 0.001$, compared to the untreated MoDC group.

GILZ expression was rapidly down-regulated as monocytes differentiated into immature MoDCs

Freshly isolated $CD14^+$ monocytes expressed GILZ at high levels, but rapidly down-regulated GILZ expression by more than 99% as they differentiated into immature MoDCs in the presence of GM-CSF and IL-4 (**Figure 1A**, $p < 0.001$). Expression of GILZ remained low in immature MoDCs for at least 72 hr in culture with no additional cytokines added. The reduction in GILZ mRNA was confirmed by a 61% decrease in intracellular GILZ protein level, as assessed by flow cytometric staining (**Figure 1B**, $p < 0.01$). Down-regulation of GILZ mRNA and protein level was correlated with reduced expression of CD14, a monocyte-specific marker (89) (**Figure 1B**, $p < 0.01$), and increased expression of cytoplasmic CD83, a marker of immature MoDCs (90) (**Figure 1B**, $p < 0.01$). HLA-DR expression also increased after 36 hr of culture, with the median fluorescent intensity (MFI) increasing from 22.8 to 149.7 ($p < 0.01$), and the percentage of $CD11c^+$ cells displaying a HLA-DR^+/cytoplasmic $CD83^+$ phenotype increasing from 15.0 ± 11.6% to 90.8 ± 5.5% ($p < 0.01$). Importantly, MoDCs remained phenotypically immature after 36 hr of culture, with a statistically insignificant change in expression of membrane CD83, a marker of mature MoDCs (90) (**Figure 1B**, $p = 0.16$).

As previously reported (59), dexamethasone induced the expression of GILZ in immature MoDCs in a dose-dependent fashion, starting at a dexamethasone concentration of 10 nM (**Figure 1C**, $p < 0.05$). Treatment with 100 nM dexamethasone for 24 hr was selected as the positive control for inducing GILZ expression in MoDCs for all future experiments (now referred to as Dex-DCs). In addition, after a single dose of 100 nM dexamethasone, GILZ was up-regulated 3.9-fold above untreated MoDCs for at least 72 hr in culture, reflecting temporal stability of GILZ up-regulation (**Figure 1F**, $p < 0.05$). This observation enabled further experiments to operate on 48 hr time scales with a single administration of dexamethasone at the initiation of cell culture.

4.2. Figure 2

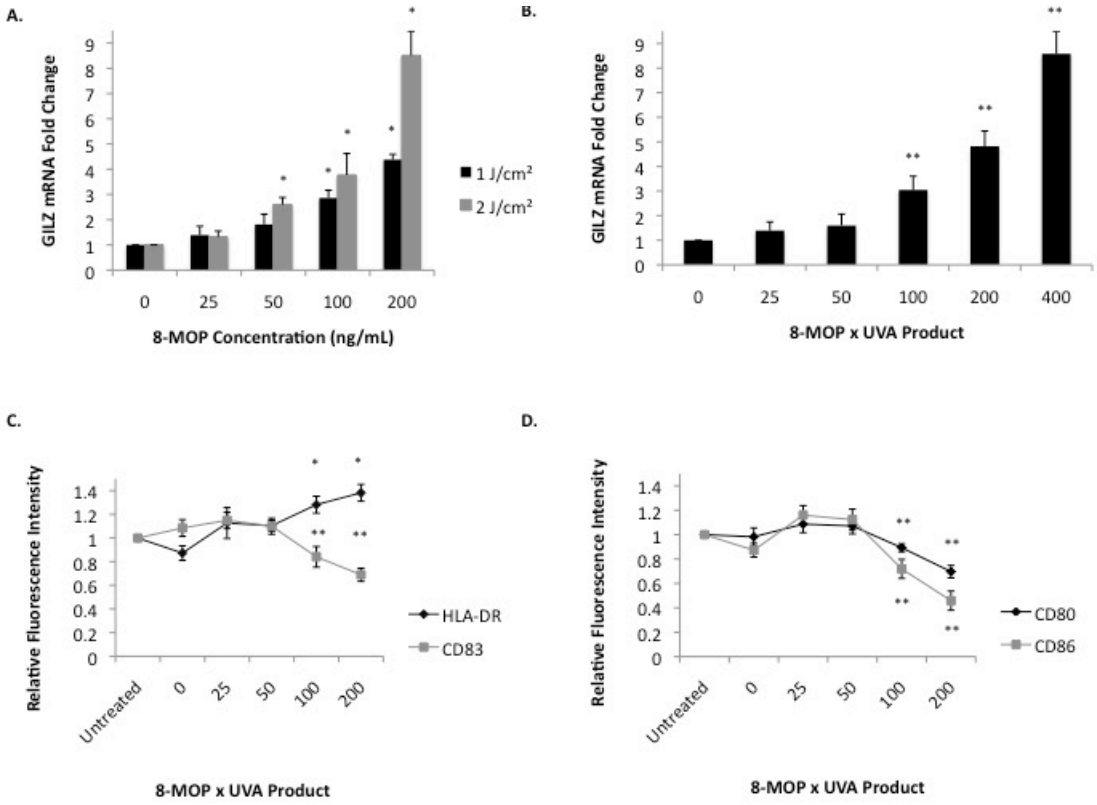

Figure 2: Immature MoDCs treated with 8-MOP plus UVA light up-regulated GILZ in a dose-dependent fashion and acquired a tolerogenic phenotype. Total RNA was isolated from MoDCs treated with PUVA. **A.)** GILZ mRNA expression is presented as a function of the 8-MOP concentration at UVA light doses of 1 J/cm^2 and 2 J/cm^2. GILZ mRNA expression in CD11c$^+$ MoDCs 24 hr after PUVA treatment is presented as a fold change relative to MoDCs receiving no 8-MOP. **B.)** GILZ mRNA expression is presented as a function of the 8-MOP concentration multiplied by the UVA light dose. GILZ mRNA expression in CD11c$^+$ MoDCs 24 hr after PUVA treatment is presented as a fold change relative to MoDCs receiving no PUVA. Relative fluorescence intensities for membrane expression of **C.)** HLA-DR and CD83, and **D.)** CD80 and CD86, are presented as a function of the 8-MOP concentration (0 to 200 ng/mL) multiplied by the UVA light dose (1 or 2 J/cm^2), 24 hr after PUVA treatment in CD11c$^+$-gated MoDCs. Untreated MoDCs served as reference controls. All data represent mean ± standard deviation for at least 4 independent experiments. For differential gene expression, a ≥ 2.5-fold change was chosen as the lower limit for considering statistically significant gene induction. *$p < 0.05$, **$p < 0.01$, compared to the untreated MoDC group.

4.3. Table 1

		Relative Fluorescence Intensity			
UVA Dose	8-MOP (ng/mL)	CD80	CD86	CD83	HLA-DR
1 J/cm^2	0	1.03 ± 0.01	1.04 ± 0.06	1.01 ± 0.64	0.96 ± 0.03
	25	1.06 ± 0.09	1.13 ± 0.20	1.11 ± 0.10	1.14 ± 0.11
	50	1.07 ± 0.11	1.10 ± 0.23	0.93 ± 0.10	1.13 ± 0.04
	100	0.93 ± 0.02	0.83 ± 0.14	0.80 ± 0.09	1.39 ± 0.13
	200	0.82 ± 0.09	0.53 ± 0.19	0.77 ± 0.05	1.06 ± 0.19
2 J/cm^2	0	1.04 ± 0.01	1.08 ± 0.06	1.46 ± 0.64	0.94 ± 0.09
	25	0.88 ± 0.12	0.89 ± 0.16	0.93 ± 0.18	1.07 ± 0.19
	50	0.89 ± 0.14	0.68 ± 0.20	0.82 ± 0.13	1.10 ± 0.25
	100	0.85 ± 0.05	0.83 ± 0.10	0.86 ± 0.06	1.17 ± 0.07
	200	0.60 ± 0.14	0.33 ± 0.34	0.54 ± 0.09	0.53 ± 0.18
Dexamethasone (100 nM)		0.92 ± 0.03	0.50 ± 0.12	0.69 ± 0.11	1.04 ± 0.11

Table 1: 8-MOP plus UVA light induced a tolerogenic phenotype in immature MoDCs in a PUVA dose-dependent fashion.
Individual relative fluorescence intensities for membrane expression of CD80, CD86, CD83 and HLA-DR are presented as a function of the 8-MOP concentration (0 to 200 ng/mL) at both 1 and 2 J/cm^2 UVA light in CD11c$^+$-gated MoDCs. Untreated MoDCs served as reference controls. All data represent mean ± standard deviation for at least 4 independent experiments. Boxes shaded in dark grey indicate statistically significant changes from untreated MoDCs, with $p < 0.05$.

The combination of 8-MOP and UVA light directly induced GILZ expression and established a tolerogenic phenotype in MoDCs

We next examined if PUVA has a direct effect on GILZ expression in immature MoDCs. Treatment with 100 ng/mL 8-MOP or 1 J/cm^2 UVA light alone did not significantly change GILZ expression (**Figure 1E**, $p > 0.05$). However, when MoDCs were treated with the combination of 100 ng/mL 8-MOP and 1 J/cm^2 UVA light (now referred to as PUVA-DCs), GILZ expression increased 5.5-fold in comparison to MoDCs receiving no PUVA treatment (**Figure 1E**, $p < 0.05$). The induction of GILZ in PUVA-DCs exhibited a slower time course in comparison to Dex-DCs, peaking 24 hr after

treatment with a 4.3-fold change above untreated MoDCs, and remaining significantly elevated, above a 3-fold change, for 72 hr in culture (**Figure 1F**, $p < 0.05$). In contrast, the induction of GILZ in Dex-DCs peaked in as little as 2 hr after dexamethasone treatment with an 8.7-fold change above untreated MoDCs, and remained significantly elevated for 72 hr in culture (**Figure 1F,** $p < 0.05$). The percentage of apoptotic cells did not differ after treatment with 100 ng/mL 8-MOP or 1 J/cm^2 UVA light, as compared to untreated MoDCs (**data not shown**). There was also no significant difference in the total number of cells recovered from any group, and greater than 90% of CD11c$^+$ MoDCs remained viable 24 hr after treatment with 100 ng/mL 8-MOP, 1 J/cm^2 UVA light, or the combination of both (**data not shown**).

After establishing that PUVA induces GILZ expression, we examined if there was an 8-MOP or UVA light dose-dependent effect on GILZ induction. MoDCs treated with 1 J/cm^2 UVA light up-regulated GILZ 2.9- and 4.4-fold higher than untreated MoDCs as the 8-MOP concentration reached therapeutic doses of 100 and 200 ng/mL respectively (**Figure 2A**, $p < 0.01$). A similar dose-dependent phenomenon was observed with 2 J/cm^2 UVA light, starting at a lower 8-MOP dose of 50 ng/mL (**Figure 2A**, $p < 0.01$).

In vivo studies utilizing highly specific 8-MOP photo-adduct monoclonal antibodies in human lymphocytes revealed that the number of photo-adducts formed per one million base pairs is directly proportional to the product of the 8-MOP concentration and UVA light dose (91). When examining GILZ expression as a function of the 8-MOP and UVA light product, a similar dose-dependent effect was observed. GILZ was up-regulated 3-fold above untreated MoDCs as the product of 8-MOP and UVA light reached 100, and 4.8- and 8.6-fold as the product increased to 200 and 400 respectively

(**Figure 2B**, $p < 0.01$). Treatment with 0.5 J/cm^2 UVA light had no significant effect on GILZ expression until the 8-MOP dose was greater than 200 ng/mL (**data not shown**). Treatment with 4 J/cm^2 UVA light resulted in high levels of non-specific cell death post-treatment, and the effects of this higher UVA light dose on GILZ expression could not be reliably determined (**data not shown**).

In dexamethasone-treated cultures, expression of GILZ truncates DC maturation and mediates the conversion to a tolerogenic phenotype (92). In a similar fashion, the PUVA dose-dependent induction of GILZ was correlated with decreased cell surface expression of the maturation marker membrane CD83 (**Figure 2C**, $p < 0.01$), and the co-stimulatory molecules CD80 and CD86 (**Figure 2D**, $p < 0.01$), in CD11c$^+$-gated MoDCs. Down-regulation of these markers paralleled the induction of GILZ (**see Figure 2B**), beginning at an 8-MOP concentration of 100 ng/mL for UVA light doses of 1 and 2 J/cm^2. As the product of 8-MOP and UVA light exceeded 100, the expression of CD83, CD80 and CD86 were reduced by 31%, 30% and 54% respectively (**Figure 2C, 2D**, $p < 0.01$), and the expression of HLA-DR was increased by 38% (**Figure 2C, 2D**, $p < 0.05$).

These same trends were observed when examining the relative fluorescence intensities (RFIs) for each cell surface marker, at each particular dose of 8-MOP and UVA light in CD11c$^+$-gated MoDCs. As the 8-MOP concentration increased at both 1 and 2 J/cm^2 UVA light, the RFIs for CD80, CD86 and CD83 all steadily decreased, in a similar fashion as Dex-DCs (**Table 1**, $p < 0.05$). Although the expression of HLA-DR increased at 100 ng/mL 8-MOP for both 1 and 2 J/cm^2 UVA light, it dropped precipitously at a dose of 200 ng/mL 8-MOP and 2 J/cm^2 UVA light (**Table 1**, $p < 0.05$).

Greater than 90% (range 91.0-97.5%) of $CD11c^+$ MoDCs were harvested from all cultures after treatment with the range of PUVA doses tested.

4.4. Figure 3

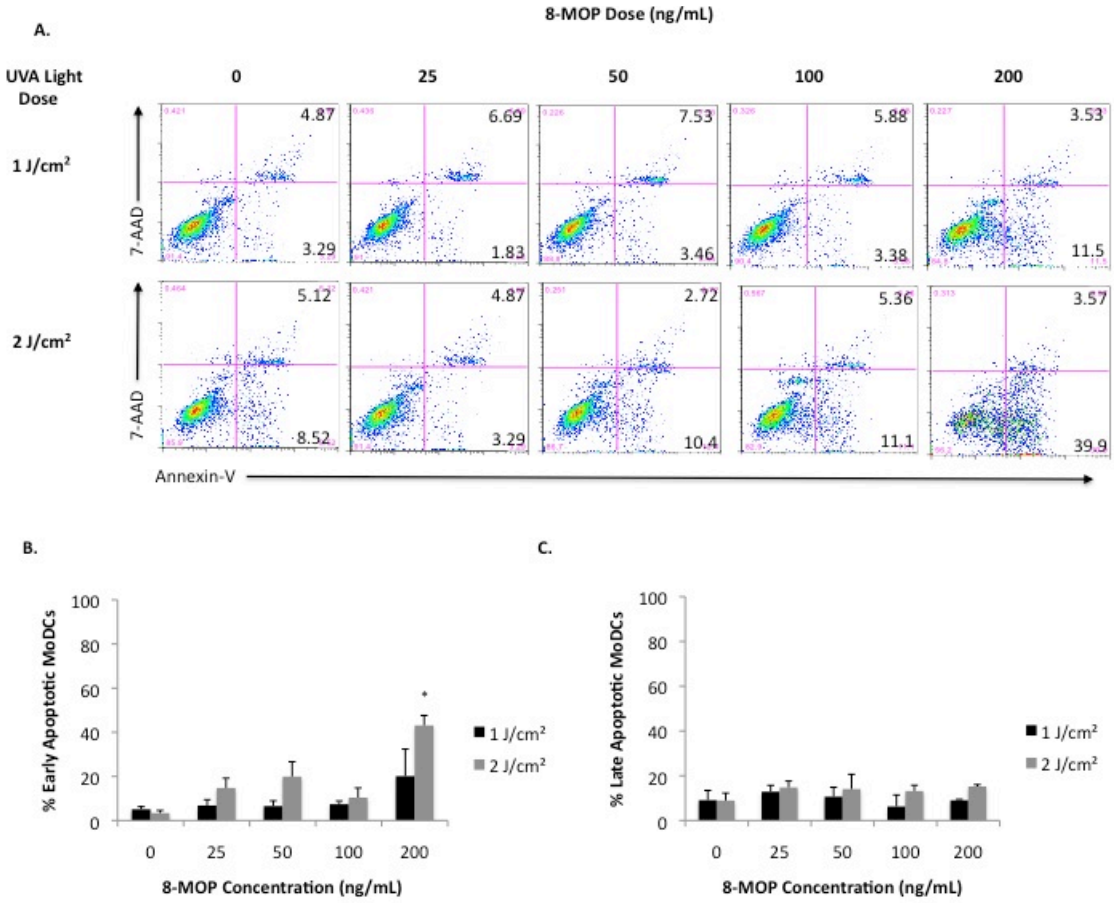

Figure 3: MoDCs were relatively resistant to the apoptotic effects of 8-MOP plus UVA light.
A.) Flow cytometry dot plots of $CD11c^+$-gated MoDCs treated with UVA light doses of 1 J/cm^2 or 2 J/cm^2, and increasing concentrations of 8-MOP, are shown for 1 representative experiment of 4. The percentages of $CD11c^+$ cells displaying Annexin-V^+/7-AAD^- (early apoptotic) or Annexin-V^+/7-AAD^+ (late apoptotic) phenotypes are indicated. The percentages of **B.)** Annexin-V^+/7-AAD^- (early apoptotic) and **C.)** Annexin-V^+/7-AAD^+ (late apoptotic) phenotypes are quantified and presented as a function of the 8-MOP concentration and UVA dose. Untreated cells served as reference controls. All data represent mean ± standard deviation for at least 4 independent experiments. *$p < 0.05$, compared to the untreated MoDC group.

4.5. Figure 4

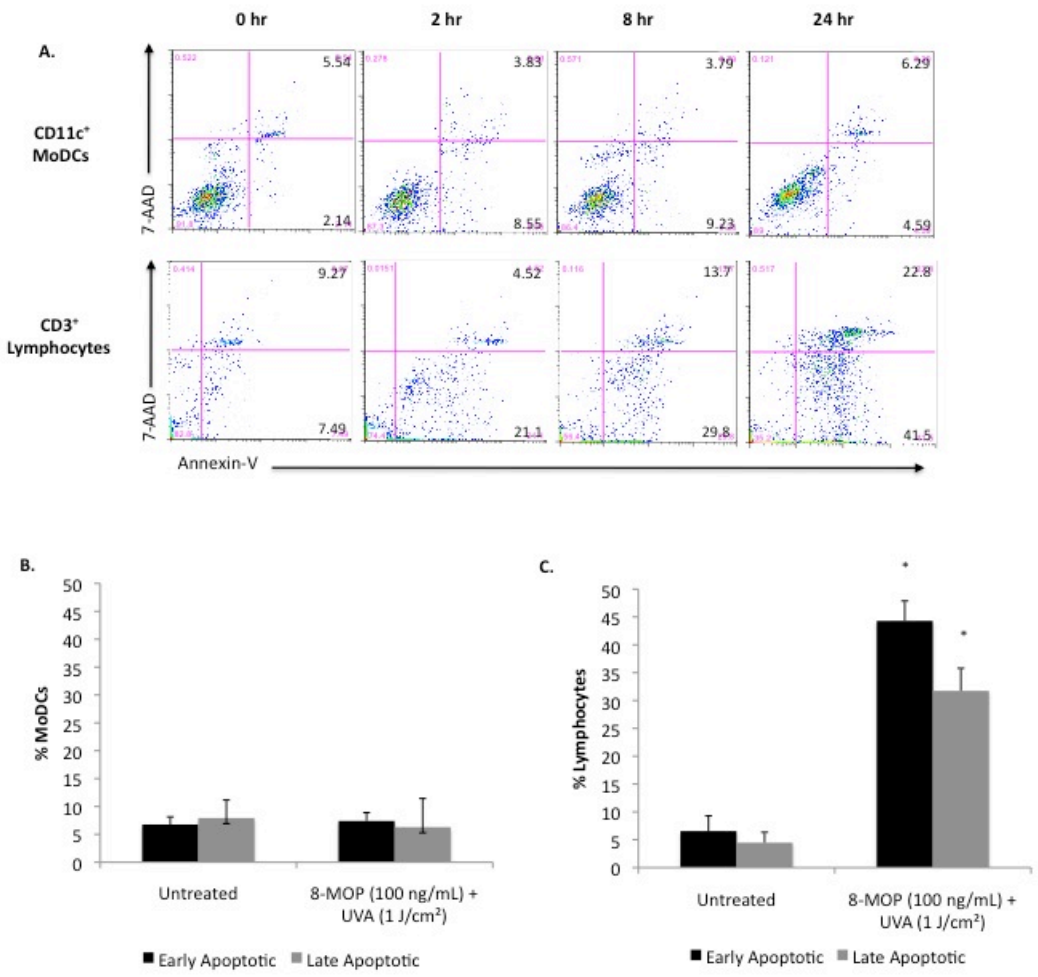

Figure 4: MoDCs and lymphocytes differed in their susceptibility to the apoptotic effects of 8-MOP plus UVA light.
A.) Flow cytometry dot plots of $CD11c^+$-gated MoDCs and $CD3^+$-gated lymphocytes treated with a UVA light dose of 1 J/cm^2, and increasing concentrations of 8-MOP, are shown for 1 representative experiment of 3. The percentages of $CD11c^+$ MoDCs displaying an Annexin-V^+/7-AAD^- (early apoptotic) or Annexin-V^+/7-AAD^+ (late apoptotic) phenotype are indicated at 0, 2, 8 and 24 hr. The percentages of **B.)** $CD11c^+$ MoDCs and **C.)** $CD3^+$ lymphocytes expressing early and late apoptotic cell markers were quantified 24 hr after treatment with 100 ng/mL 8-MOP and 1 J/cm^2 UVA light. Untreated MoDCs and lymphocytes served as reference controls. All data represent mean ± standard deviation for at least 3 independent experiments. *$p < 0.05$, compared to the untreated MoDC or lymphocyte group.

Lymphocytes were particularly susceptible, whereas MoDCs were relatively resistant, to the apoptotic effects of PUVA

There is a lack of consensus in the literature regarding the apoptotic effects of PUVA treatment on monocytes and DCs, with studies showing both a resistance (12, 21-23), and sensitivity (24-26), to apoptosis. The relative resistance of MoDCs to the apoptotic effects of PUVA can be directly observed on flow cytometry dot plots from 1 representative experiment of 4 (**Figure 3A**). The percentage of early apoptotic (Annexin-V^+/7-AAD^-) $CD11c^+$-gated MoDCs was minimally higher when treated with 2 J/cm^2 as compared to 1 J/cm^2 UVA light, across the range of 8-MOP concentrations tested (0 to 200 ng/mL) (**Figure 3A**, $p > 0.05$). Of note, there was a statistically significant increase in the percentage of early apoptotic $CD11c^+$-gated MoDCs when treated with 2 J/cm^2 UVA light and 200 ng/mL 8-MOP, as compared to untreated MoDCs (**Figure 3A, 3B**, $p < 0.05$). Nevertheless, apart from this isolated PUVA dose, the percentage of early apoptotic MoDCs remained below 25% (range 3.4-20.2%) over the range of 8-MOP and UVA light doses examined (**Figure 3B**, $p > 0.05$).

The percentage of late apoptotic (Annexin-V^+/7-AAD^+) $CD11c^+$-gated MoDCs also remained low (range 6.3-15.2%), and statistically not different than untreated MoDCs, at both 1 J/cm^2 and 2 J/cm^2 UVA light for all concentrations of 8-MOP tested (**Figure 3C**, $p > 0.05$). Moreover, greater than 90% $CD11c^+$ MoDCs (range 91.0-97.5%) were harvested after PUVA treatment from all groups treated with 1 or 2 J/cm^2 UVA light.

In comparison to MoDCs, $CD3^+$-gated lymphocytes displayed phosphatidylserine on their cell surface as early as 2 hr after treatment with 1 J/cm^2 UVA light and 100 ng/mL 8-MOP (**Figure 4A**). As directly observed on flow cytometry dot plots from 1

representative experiment of 3, 2 hr after treatment with 1 J/cm^2 UVA light and 100 ng/mL 8-MOP, the percentage of early apoptotic CD3$^+$-gated lymphocytes increased from 7.5% to 21.1% (**Figure 4A**). Moreover, the percentage of early and late apoptotic CD3$^+$-gated lymphocytes further increased at both 8 and 24 hr (**Figure 4A**). In comparison, there was no significant increase in the percentage of early or late apoptotic CD11c$^+$-gated MoDCs after treatment with the same dose of 8-MOP and UVA light at 2, 8 or 24 hr (**Figure 4A**).

Figures 4B and 4C quantify the striking difference in susceptibility of MoDCs and lymphocytes to an identical 8-MOP and UVA light dose. While there were no differences observed in the percentages of early or late apoptotic CD11c$^+$-gated MoDCs 24 hr after treatment with 100 ng/mL 8-MOP and 1 J/cm^2 UVA light (**Figure 4B**, $p > 0.05$), there was a large increase in the percentage of early and late apoptotic lymphocytes 24 hr after PUVA treatment (**Figure 4C**, $p < 0.05$). The percentage of early apoptotic lymphocytes increased from 6.6% in untreated lymphocytes to 44.3% in PUVA-treated lymphocytes, and the percentage of late apoptotic lymphocytes increased from 4.5% to 33.7% (**Figure 4C**, $p < 0.05$). Given that 64.3 ± 3.2% ($p < 0.001$) of CD3$^+$-gated lymphocytes displayed phosphatidylserine on their cell surface and were apoptotic 24 hr after PUVA treatment, PUVA-treated lymphocytes are subsequently referred to as apoptotic lymphocytes (ApoL).

4.6. Figure 5

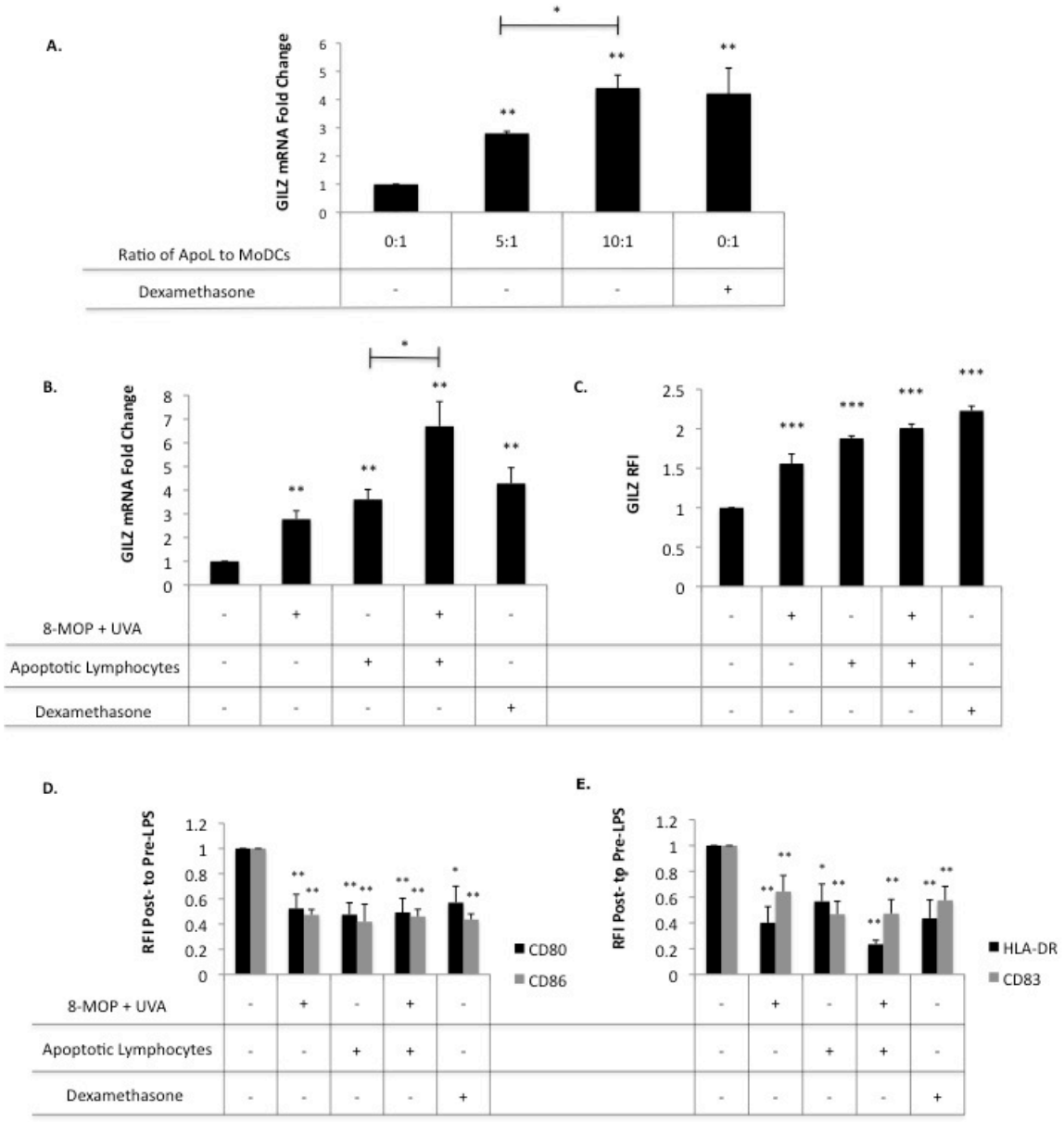

Figure 5: Immature MoDCs exposed to apoptotic lymphocytes up-regulated GILZ and were resistant to full maturation with LPS.
A.) GILZ mRNA expression in $CD11c^{+}$ MoDCs 24 hr after co-culture is presented as a fold change relative to untreated MoDCs that were cultured alone. MoDCs were co-cultured in ratios of five and ten apoptotic lymphocytes to one untreated MoDC. **B.)** GILZ mRNA expression in $CD11c^{+}$ MoDCs 24 hr after co-culture is presented as a fold

change relative to untreated MoDCs that were cultured alone. **C.)** Relative fluorescence intensity of GILZ 24 hr after co-culture. Relative fluorescence intensities post- to pre-LPS stimulation for **D.)** CD80 and CD86, and **E.)** HLA-DR and CD83, were calculated as follows: $(MFI_{\text{treated after LPS}} - MFI_{\text{treated before LPS}}) / (MFI_{\text{untreated after LPS}} - MFI_{\text{untreated before LPS}})$. Data represent mean ± standard deviation for at least 4 independent experiments. For differential gene expression, a ≥ 2.5-fold change was chosen as the lower limit for considering statistically significant gene induction. $*p < 0.05$, $**p < 0.01$, $***p < 0.001$, compared to the untreated MoDC group, unless noted otherwise.

MoDCs exposed to apoptotic lymphocytes increased expression of GILZ and were resistant to full maturation after LPS stimulation

To dissect the direct effects of PUVA on MoDCs, and the indirect effects of PUVA through the generation of ApoL, immature MoDCs were co-cultured for 24 hr with increasing numbers of ApoL. Exposure of MoDCs to ApoL induced GILZ expression in an ApoL dose-dependent fashion, with GILZ expressed higher in MoDCs co-cultured in a ten to one ratio of ApoL to MoDCs as compared to a five to one ratio (4.4-fold compared to 2.8-fold higher than untreated MoDCs, respectively) (**Figure 5A**, $p < 0.01$). As a positive control, dexamethasone induced GILZ expression 4.2-fold above untreated MoDCs in this particular set of experiments (**Figure 5A**, $p < 0.01$).

In addition, PUVA-DCs co-cultured with ApoL expressed GILZ at higher levels than PUVA-DCs cultured alone (6.7-fold compared to 2.8-fold higher than untreated MoDCs, respectively) (**Figure 5B**, $p < 0.05$). PUVA-DCs exposed to ApoL also expressed GILZ at higher levels than did untreated MoDCs exposed to ApoL (6.7-fold compared to 3.6-fold higher than untreated MoDCs, respectively) (**Figure 5B**, $p < 0.01$). Increased GILZ mRNA production was associated with at least a 1.5-fold increase (range 1.56-2.23) in the intracellular level of GILZ protein (**Figure 5C**, $p < 0.001$). The induction of GILZ was not related to an increase in the number of early or late apoptotic cells, as there were less than 12% early apoptotic (range 3.8-11.4%) and 12% late

apoptotic (range 6.3-11.5%) $CD11c^+$ MoDCs in all groups demonstrating induction of GILZ ($p > 0.05$, as compared to untreated MoDCs).

Immature MoDCs exposed to LPS rapidly mature and increase membrane expression of HLA-DR, CD83, CD80 and CD86 (93). MoDCs expressing GILZ greater than 2.5-fold above untreated MoDCs were resistant to full maturation by the TLR4 ligand LPS, and acquired a semi-mature, tolerogenic phenotype. LPS stimulation increased CD80 expression in MoDCs up-regulating GILZ to only 50% (range 48-57%) of the levels seen after LPS stimulation in untreated MoDCs (**Figure 5D**, $p < 0.05$), and LPS stimulation increased CD86 expression to only 45% (range 42-47%) of untreated MoDCs (**Figure 5D**, $p < 0.01$). Similar results were obtained for CD83 (range 47-65%) and HLA-DR (range 23-57%), as compared to untreated MoDCs after LPS stimulation (**Figure 5E,** $p < 0.05$). The reduction in cell surface marker expression was confirmed at the mRNA level for CD80 and CD86, as assessed by qRT-PCR. MoDCs up-regulating GILZ expressed 6% of the CD80 mRNA transcript level of untreated MoDCs (range 4.5-7.5%, $p < 0.05$) and expressed 50% of the CD86 mRNA transcript level of untreated MoDCs (range 12.4-85.1%, $p < 0.05$). MoDCs not stimulated with LPS served as negative controls, and demonstrated baseline expression levels for all cell surface markers, and also had low transcript levels for both CD80 and CD86 mRNA (**data not shown**).

4.7. Figure 6

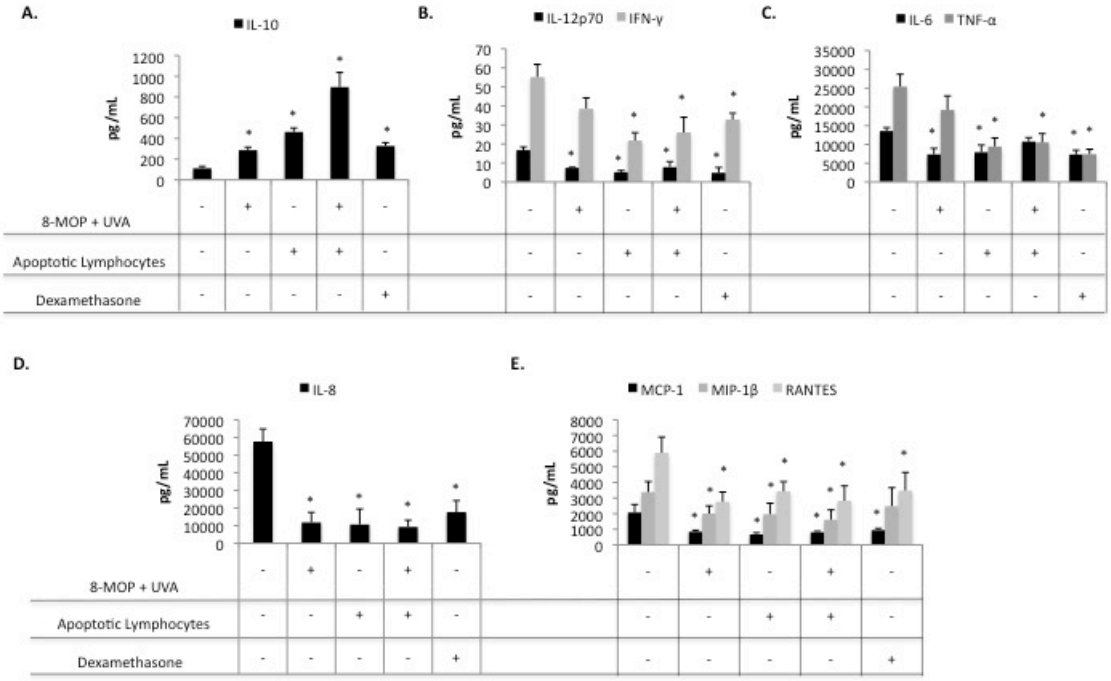

Figure 6: MoDCs up-regulating GILZ at high levels increased IL-10 production, and decreased production of various pro-inflammatory cytokines and chemokines. MoDCs from cultures described in Figure 5 were stimulated with LPS, and after 24 hr culture supernatants were harvested for cytokine quantification by magnetic bead multiplex immunoassays for **A.)** IL-10, and the pro-inflammatory cytokines **B.)** IL-12p70 and IFN-γ, and **C.)** IL-6 and TNF-α. The same analysis was performed for the pro-inflammatory chemokines **D.)** IL-8, and **E.)** MCP-1, MIP-1β and RANTES. Data are presented as mean ± standard deviation for 3 independent experiments. $*p < 0.05$ compared to the untreated MoDC group.

4.8. Figure 7

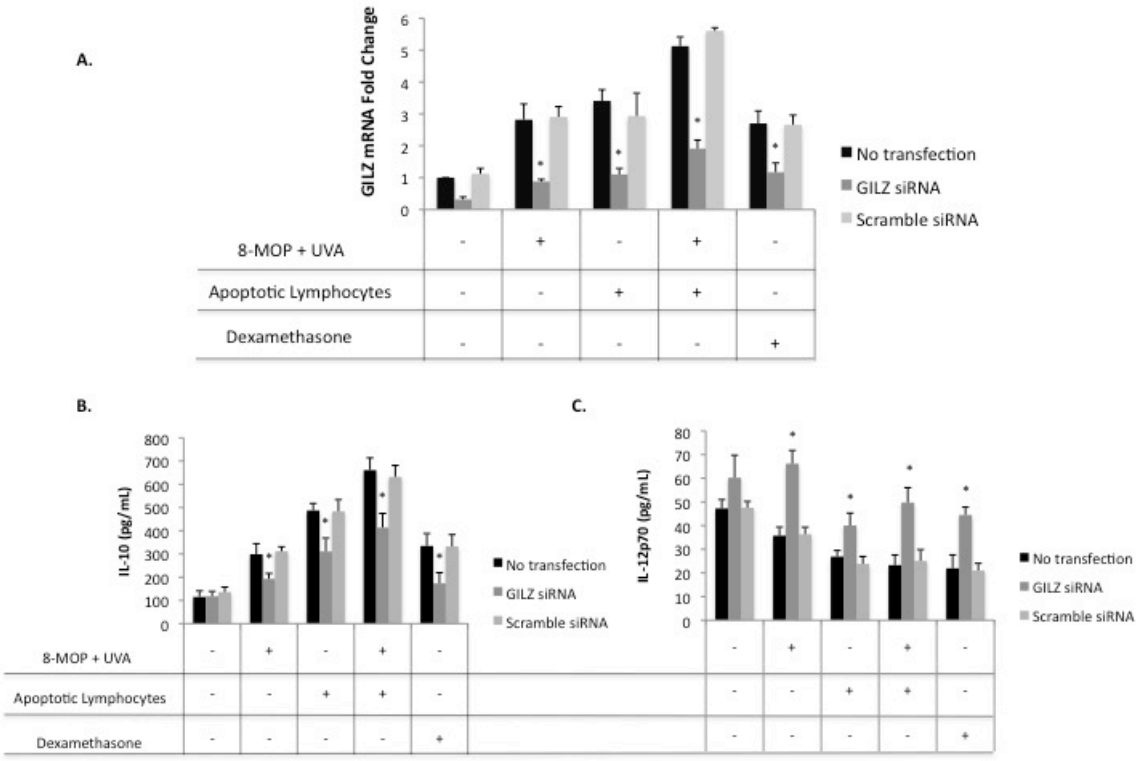

Figure 7: siRNA-mediated knockdown of GILZ abolished the tolerogenic cytokine profile, as evidenced by reduced IL-10 production and increased IL-12 production. MoDCs were transfected with GILZ or scramble siRNA, and cultured as described in Figure 5. **A.)** GILZ mRNA expression in $CD11c^{+}$ MoDCs transfected with GILZ or scramble siRNA is presented as a fold change compared to non-transfected, untreated MoDCs that were cultured alone. * ≥ 2.5-fold change and $p < 0.05$, compared to identically treated MoDCs not transfected with siRNA. Quantification of **B.)** IL-10 and **C.)** IL-12p70 protein levels in culture supernatants 24 hr after LPS stimulation. Data represent mean ± standard deviation for 3 independent experiments**.** *$p < 0.05$, compared to identically treated MoDCs not transfected with siRNA.

4.9. Table 2

	Non-Transfected			GILZ siRNA		
	IL-10 (ng/mL)	IL-12p70 (ng/mL)	IL-10/IL-12	IL-10 (ng/mL)	IL-12p70 (ng/mL)	IL-10/IL-12
Untreated MoDCs	115.2 ± 26.0	47.3 ± 3.7	5.0	117.7 ± 21.4	60.2 ± 9.5	2.0
PUVA-DCs	299.0 ± 45.3	35.8 ± 3.6	8.4	193.1 ± 23.2	66.2 ± 5.6	2.9
Untreated MoDCs + ApoL	487.5 ± 30.0	26.9 ± 2.6	18.1	310.9 ± 57.4	40.0 ± 5.3	7.8
PUVA-DCs + ApoL	661.2 ± 52.3	23.3 ± 4.3	28.4	413.6 ± 61.1	49.7 ± 6.3	8.3
Dex-DCs	334.7 ± 53.4	21.9 ± 5.7	15.3	173.7 ± 45.5	44.5 ± 3.3	3.9

Table 2: MoDCs expressing GILZ at high levels demonstrated an increased IL-10 to IL-12 ratio characteristic of tolerogenic DCs, and siRNA-mediated knockdown of GILZ reduced the IL-10 to IL-12 ratio.
GILZ mRNA expression in $CD11c^+$ MoDCs is presented as a fold change relative to untreated MoDCs that were cultured alone. Individual IL-10 and IL-12 levels are presented, with a calculation of the IL-10 to IL-12 ratio for each group. Data represent mean ± standard deviation for 3 independent experiments. Shaded boxes highlight the IL-10 to IL-12 ratio for each group.

MoDCs expressing high levels of GILZ displayed a tolerogenic cytokine profile, and siRNA-mediated knockdown of GILZ reduced the IL-10 to IL-12 ratio

Tolerogenic DCs are characterized by increased production of immunosuppressive cytokines and decreased production of pro-inflammatory cytokines and chemokines (36, 40-42). To analyze the functionality of MoDCs expressing GILZ at high levels, supernatants were harvested from the co-cultures described in Figure 5B. Dex-DCs expressed GILZ 4.29-fold above untreated MoDCs (**see Figure 5B**, $p < 0.01$), and in comparison to untreated MoDCs, increased production of the immunosuppressive cytokine IL-10 (**Figure 6A**, $p < 0.05$). In addition, Dex-DCs decreased production of the pro-inflammatory cytokines IL-12p70 and IFN-γ (**Figure 6B**, $p < 0.05$), IL-6 and TNF-α

(**Figure 6C**, $p < 0.05$), and chemokines IL-8 (**Figure 6D**, $p < 0.05$), and MCP-1 and RANTES (**Figure 6E**, $p < 0.05$). Dex-DCs did not, however, significantly decrease production of the chemokine MIP-1β (**Figure 6E**, $p > 0.05$).

PUVA-DCs expressed GILZ 2.78-fold above untreated MoDCs (**see Figure 5B**, $p < 0.01$), and in comparison to untreated MoDCs, increased production of IL-10 (**Figure 6A**, $p < 0.05$). PUVA-DCs also decreased production of IL-12p70, IL-6, IL-8, MCP-1, MIP-1β and RANTES (**Figure 6B-6E**, $p < 0.05$), but not TNF-α or IFN-γ (**Figure 6B, 6C**, $p > 0.05$). As previously noted, both PUVA-DCs and untreated MoDCs, when co-cultured with ApoL, expressed GILZ at higher levels that PUVA-DCs cultured alone (3.6- and 6.7-fold higher, respectively) (**see Figure 5B,** $p < 0.01$). In comparison to untreated MoDCs, these two groups both increased production of IL-10 (**Figure 6A,** $p < 0.05$), and decreased production of the pro-inflammatory cytokines IL-12p70, IFN-γ, IL-6 and TNF-α (**Figure 6B, 6C**, $p < 0.05$**)** and chemokines IL-8, MCP-1, MIP-1β and RANTES (**Figure 6D, 6E,** $p < 0.05$).

Cytokine levels were also analyzed at the RNA level for IL-10, IL-12, TNF-α and TGF-β, as assessed by qRT-PCR. MoDCs that significantly up-regulated GILZ 2.5-fold above untreated MoDCs also up-regulated IL-10 mRNA transcripts to levels 8-fold greater than untreated MoDCs (range 5.5-11.8 fold higher, $p < 0.01$). Moreover, these MoDCs down-regulated IL-12 mRNA transcripts to levels 1.7-fold lower than MoDCs (range 1.1-3.2 fold lower, $p < 0.05$), and down-regulated TNF-α mRNA transcripts to levels 1.4-fold lower than MoDCs (range 1.1-2.0 fold lower, $p > 0.05$). In addition, TGF-β mRNA was up-regulated in PUVA-DCs 3.4-fold above untreated MoDCs (range 2.2-4.6 fold higher, $p < 0.05$), and in PUVA-DCs exposed to ApoL, TGF-β mRNA was up-

regulated 3.0-fold above untreated MoDCs (range 2.9-3.0 fold higher, $p < 0.05$). In untreated MoDCs exposed to ApoL, TGF-β was marginally up-regulated only 2.1-fold above untreated MoDCs (range 1.2-3.0 fold higher, $p > 0.05$), and TGF-β mRNA transcripts were actually lower in Dex-DCs (0.8-fold lower in comparison to untreated MoDCs) (range 0.8-0.9 fold lower, $p > 0.05$). Of note, TGF-β was not included in the multiplex cytokine analysis and therefore was only analyzed at the mRNA level.

To assess whether the induction of GILZ was mediating the observed tolerogenic cytokine profile, MoDCs were transfected with GILZ specific-siRNA to transiently knockdown GILZ expression. Transfection with GILZ siRNA reduced GILZ expression in MoDCs by 65% (range 57-69%, of non-transfected MoDCs) (**Figure 7A**, $p < 0.05$). Transfection with scramble siRNA did not significantly change GILZ expression (range 86-112% of non-transfected MoDCs) (**Figure 7A,** $p > 0.05$). There was no significant difference in the number of cells recovered from any group transfected with siRNA as compared to non-transfected groups (**data not shown,** $p > 0.05$). MoDCs up-regulating GILZ 2.5-fold higher than untreated MoDCs, in both the non-transfected and scramble siRNA groups, produced higher levels of IL-10 (**Figure 7B**, $p < 0.05$). Transient knockdown of GILZ reduced IL-10 production by 39% (range 34-48%) (**Figure 7B**, $p < 0.05$). MoDCs up-regulating GILZ 2.5-fold higher than untreated MoDCs in both the non-transfected and scramble siRNA groups also produced lower levels of IL-12p70 (**Figure 7C**, $p < 0.05$). Transient knockdown of GILZ increased IL-12p70 production by 188% (range 149-214%) (**Figure 7C**, $p < 0.05$). Treatment with scramble siRNA had no appreciable effect on the production of either IL-10 or IL-12p70 (**Figure 7B, 7C**, $p > 0.05$).

The ratio of IL-10 to IL-12 production is a useful indicator of tolerogenicity, and tolerogenic DCs are characterized by an increased IL-10 to IL-12 ratio (36, 40-42). The IL-10 to IL-12 ratio increased from 5.0 in untreated MoDCs to 15.3 in Dex-DCs (**Table 2**). Similarly, the IL-10 to IL-12 ratio increased to 8.4 in PUVA-DCs, increased to 18.1 in untreated MoDCs exposed to ApoL, and increased to 28.4 in PUVA-DCs exposed to ApoL (**Table 2**).

Transient knockdown of GILZ with siRNA reduced the IL-10 to IL-12 ratio that had been elevated following GILZ induction. The IL-10 to IL-12 ratio decreased from 15.3 to 3.9 in siRNA transfected Dex-DCs (**Table 2**). Similarly, in siRNA transfected PUVA-DCs, the ratio decreased from 8.4 to 2.9, in siRNA transfected untreated MoDCs exposed to ApoL, the ratio decreased from 18.1 to 7.8, and finally in siRNA transfected PUVA-DCs exposed to ApoL, the ratio decreased from 28.4 to 8.3 (**Table 2**, $p < 0.05$).

Discussion

5.1. Summary of Results

This study demonstrates that PUVA acts directly on MoDCs, and indirectly through the generation of ApoL, to induce expression of GILZ. MoDCs up-regulating GILZ displayed a tolerogenic phenotype, characterized by moderate expression of the MHC-class II molecule HLA-DR, low expression of the co-stimulatory molecules CD80 and CD86, and low expression of the maturation marker CD83. Moreover, MoDCs up-regulating GILZ were resistant to full maturation by the TLR4 ligand LPS, indicating that they were in a tolerogenic, semi-mature state, unable to mature and respond to classic immunogenic stimuli.

In addition, MoDCs treated with PUVA, or exposed to lymphocytes rendered apoptotic by PUVA, were polarized towards a tolerogenic cytokine profile, characterized by increased IL-10 production and decreased production of pro-inflammatory cytokines, including IL-12, IFN-γ, IL-6 and TNF-α, and chemokines, including IL-8, MCP-1, MIP-1β, and RANTES. GILZ was necessary for the conversion to this tolerogenic cytokine profile, as demonstrated by a reduction in the IL-10 to IL-12 ratio after siRNA-mediated transient knockdown of GILZ. PUVA and apoptotic cells can now be included in the list of immunosuppressive stimuli - including glucocorticoids, IL-10 and TGF-β - all sharing GILZ induction as the common downstream mechanism mediating their tolerogenic effects.

5.2. Direct Effects of PUVA

The molecular pathways mediating PUVA's direct induction of GILZ are presently unknown, but may be related to DNA damage, protein modifications, or cellular stress. IL-10 levels were also elevated in PUVA-treated cultures, indicating that autocrine or paracrine IL-10 signaling could have been the primary event inducing GILZ expression (73). However, this is less likely given that the measured IL-10 concentration was 350 times lower than that used to induce moderate GILZ expression in prior studies (59).

While 8-MOP is biologically inert in the absence of UVA light energy, UV radiation is immunosuppressive (1, 3), and activates numerous transcription factors, including the immediate early genes c-fos, c-jun, and c-myc (94) . Moreover, transcription factor induction is observed even in DNA repair-deficient cells (94), indicating that photo-adduct repair and processing are not required for gene induction. PUVA itself also alters gene expression in mouse keratinocytes (95), and generates bulky DNA-protein cross-links (96), reactive oxygen species (97, 98), and lipid modifications (99, 100), all of which may be able to induce gene expression. Given the relative resistance of MoDCs to apoptosis, sub-lethal DNA damage and generalized cellular stress may be capable of inducing GILZ and generating tolerogenic DCs. Interestingly, IL-2 growth factor deprivation induces GILZ expression in T-lymphocytes and protects them from IL-2 withdrawal-induced apoptosis (101). PUVA may induce GILZ expression in a similar fashion, protecting MoDCs from PUVA-induced apoptosis.

Multiple studies link cellular stress with GILZ induction. Firstly, rat macrophages subjected to hypoxic conditions up-regulate GILZ in an ERK-dependent

fashion (102). Secondly, caspase-8, linked to the immediate pre-programmed apoptotic pathway induced by PUVA (16, 17), protects GILZ from degradation by facilitating its binding to the small ubiquitin-like modifier 1 (SUMO-1) (103). SUMO-1 is covalently attached to proteins during post-translational modifications, and is involved in many cellular processes, including apoptosis and the response to stress (103). The presence of SUMO binding sites on the GILZ protein suggests a close relationship between GILZ induction, cellular stress and apoptosis (103). Thirdly, a recent report suggested that treatment of mouse bone marrow derived DCs with thermal stress in the presence of carvacrol, a molecule with anti-inflammatory properties, could induce functionally tolerogenic DCs (104). Fourthly, GILZ has even been shown to be an alcohol-responsive gene, becoming up-regulated in response to ethanol in a dose-dependent manner (105). Finally, exposure to certain microbial products, including *C. difficile* toxin B and *Y. enterocolitica* virulence factor YopT, induce GILZ expression (106). The notion that cellular stress may induce a default tolerogenic pathway of DC differentiation has not been systematically explored to date. However, given the importance of maintaining peripheral tolerance to self-antigens exposed during tissue damage in times of inflammation and infection (34-36), the idea that a tolerogenic differentiation program may become activated in a subset of DCs during stressful environmental conditions warrants further investigation.

The product of the 8-MOP and UVA light dose is directly proportional to the number of photo-adducts formed per one million base pairs (91). A direct role for protein and/or DNA photo-adduct formation contributing towards GILZ induction is supported by the 8-MOP and UVA light product dose-dependent up-regulation of GILZ (see **Figure**

2B). It is interesting to note that the induction of GILZ, and down-regulation of CD80, CD86 and CD83, only occurred as the product of 8-MOP and UVA light reached therapeutic levels, namely between 100 and 200 (see **Figure 2C, 2D**). Doses of 8-MOP and UVA light used during ECP vary between treatment centers, but generally range from 1 to 2 J/cm^2 of UVA light and from 100 to 200 ng/mL of 8-MOP (7-10). Down-regulation of these markers was likely not due to the non-specific global suppression of all cell surface marker expression, as the expression level of HLA-DR increased at identical PUVA doses. In support of these data, a prior study also noted increased antigen uptake and HLA-DR expression in PUVA-treated MoDCs (53), and also enhanced MHC class I synthesis after low-dose PUVA treatment (98).

5.3. Apoptotic Effects of PUVA

In support of previously published studies (12, 21-23), MoDCs were relatively resistant to the apoptotic effects of PUVA. The discrepancy between these data, and other reports suggesting a susceptibility of MoDCs to apoptosis (24-26), may stem from variations in the PUVA dose used for treatment. For example, Holtick *et al.* reported a susceptibility of MoDC to apoptosis, but utilized both a high 8-MOP concentration (300 ng/mL) and UVA light dose (2 J/cm^2) (25). This 8-MOP and UVA light product, proportional to the extent of DNA damage, is approximately twice the therapeutic dose (7, 25). Likewise, Yoo *et al.* reported that MoDC apoptosis was observed with 8-MOP administration alone, at doses greater than 300 ng/mL (13), and with UVA light alone, at doses greater than 2 J/cm^2 (13), suggesting that very high doses of either 8-MOP or UVA light alone can also lead to non-specific cell death.

In this present study, high doses of PUVA only minimally increased the percentage of early apoptotic MoDCs. However, after treatment with a supra-therapeutic dose (2 J/cm^2 UVA light and 200 ng/mL 8-MOP), the percentage of early apoptotic MoDCs significantly increased (see **Figure 3**). The transcriptional and phenotypic changes observed at this high PUVA dose were likely non-specific, given a marked decrease in the RFIs for all cell surface markers, including HLA-DR (see **table 1**). Importantly though, no therapeutic PUVA dose used in this study increased the percentage of late apoptotic MoDCs above the levels observed with untreated MoDCs, indicating that rapid MoDC death is likely not occurring during or after ECP.

The previously documented exquisite sensitivity of lymphocytes to the apoptotic effects of PUVA was confirmed in this study (12-14). Over 60% of lymphocytes displayed phosphatidylserine on their cell surface 24 hr after PUVA treatment, and between 70% and 90% of lymphocytes entered a late stage of apoptosis 48 hr after treatment. In fact, as early as 2 hr after PUVA treatment, 21% of lymphocytes displayed phosphatidylserine, illustrating the activation of an immediate pre-programmed apoptotic pathway (16, 17).

5.4. Indirect Effects of PUVA

The transcription factor NF-κB is a key regulator of many genes associated with DC immunogenicity, and many inflammatory stimuli, such as LPS, TNF-α, and IL-1, induce DC maturation through activation of the NF-κB pathway (107). Therefore, it is not surprising that many immunosuppressive stimuli act by inhibiting NF-κB, and GILZ is a direct inhibitor of NF-κB in T-lymphocytes (72), macrophages (62), and DCs (59,

69). In addition, the exposure of DCs to apoptotic cells has been shown to inhibit NF-κB (108), leading to a truncation in DC maturation and polarization towards a tolerogenic functional state (109). This present study implicates GILZ as the downstream molecular mediator transmitting the immunosuppressive effects of apoptotic cells, ultimately resulting in NF-κB inhibition. MoDCs exposed to ApoL up-regulated GILZ in an apoptotic cell dose-dependent manner, and acquired a tolerogenic phenotype and function. The tolerogenic functional profile of these cells was diminished after transient knockdown of GILZ with siRNA.

The immunosuppressive elements associated with apoptotic cells have not been fully elucidated, but likely involve unique molecular characteristics of the apoptotic cell, the production of tolerogenic factors, the kinetics of cell death, and the nature of the apoptotic-inducing stimulus (110). Apoptotic lymphocytes display phosphatidylserine on their surface soon after apoptosis is initiated (83), and this process triggers recognition and removal by APCs (82). Receptors involved in the recognition and internalization of apoptotic bodies include phosphatidylserine receptors (TAM receptors) (84), the thrombospondin receptor (CD36) (78, 79), the vitronectine receptor ($\alpha_V\beta_3$ integrin) (74), and other scavenger receptors (78). Notably, both phosphatidylserine (79), and anti-CD36 (83), are capable of transmitting immunosuppressive signals from apoptotic cells. This suggests that the exposure of phosphatidylserine and other molecules recognized by scavenger receptors may comprise the bulk of these signals. Recently, membrane blebs containing high levels of phosphatidylserine were observed to originate from apoptotic lymphocytes after PUVA treatment,' and these membrane blebs contained an immunosuppressive surface composition of antigens' (111). It is reasonable that the

recognition and internalization of membrane blebs constituted the major immunosuppressive signal from apoptotic lymphocytes and induced GILZ expression in this study.

In addition, lymphocytes release both IL-10 (112) and TGF-β (113) as they undergo controlled apoptosis, and UV-irradiated lymphocytes have also been observed to produce IL-10 (114). It remains a possibility that GILZ induction may have resulted from IL-10 release by ApoL, with subsequent paracrine signaling within cell culture. In contrast, rapid lymphocyte apoptosis, leading to secondary necrosis, results in the release of numerous DAMPs, including high-mobility group box-1 (HMGB-1), heat shock proteins, uric acid, and mammalian DNA, all of which are highly immunogenic (110). Thus the extent of cell death and the kinetics of apoptotic induction likely play a key role in determining which types of signals are transmitted (110). Of interest, lymphocytes in this study exhibited widespread apoptotic death following PUVA exposure, but first entered through a distinct early apoptotic stage in which their cellular membranes were intact and DAMPs were presumably not released in significant quantities (see **Figure 4A)**. Moreover, there was no indication of lymphocyte necrosis preceding apoptosis, providing additional circumstantial evidence that MoDCs were capable of processing these cells efficiently before they entered stages of late apoptosis.

An additional interesting hypothesis is that reactive oxygen species generated from PUVA exposure may modify HMGB-1 and other DAMPs, abolishing their intrinsic immunogenicity once released from the dying cell (110). In support of this claim, Kazama *et al.* demonstrated that the induction of tolerance by apoptotic cells requires caspase-dependent oxidation of HMGB-1 (115). Given that PUVA activates an early

apoptotic pathway in lymphocytes involving caspase-3, -8, and -9 (15-17), apoptotic lymphocytes induced by PUVA may be uniquely conditioned to induce tolerance through the oxidation and neutralization of HMGB-1 (115). A limitation of this present study is that only the exposure of MoDCs to ApoL was linked with GILZ induction. A requirement for cell-contact between DCs and ApoL, or the contributions from internalization, release of IL-10 or DAMPs, and other signaling pathways were not fully investigated. Additional studies will be required to elucidate precisely how cell-to-cell contact, IL-10 production by PUVA-treated cells, and the internalization of apoptotic bodies contribute to the induction of GILZ.

One intriguing possibility is that TAM receptor signaling may provide the missing link between cell surface recognition of apoptotic cells and GILZ induction. TAM (Tyro3, Axl, Mer) receptors are a family of tyrosine kinases capable of transducing immunosuppressive signals from apoptotic cells (84, 116). TAM receptors were originally demonstrated to inhibit TLR-induced inflammation in a tripartite model postulated by Rothlin *et al.* (117). This model asserts that TLR ligation initially leads to the production of cytokines that promote inflammation and host defense (117). In the second part of the model, these pro-inflammatory cytokines amplify the inflammatory response through feed-forward signaling (117). In the final stage, these same cytokines induce TAM receptor activation as a negative feedback mechanism to inhibit the inflammatory response (117). This system is postulated to enable the immune system to quickly launch an immunogenic, pro-inflammatory response that is ensured to be self-limiting and non-detrimental to the host through inhibitory signaling from TAM receptor activation (117).

TAM receptors also have an important role in apoptotic cell homeostasis (84). TAM-deficient cells fail to properly internalize apoptotic cells and membranes (84), and autoimmune disease universally develops in TAM knockout mice, likely as a result of the aberrant clearance of apoptotic cells by APCs (116, 118). Growth arrest-specific 6 (GAS6) and protein S, two TAM receptor ligands produced by macrophages and DCs, bind phosphatidylserine and form a molecular bridge between the apoptotic cell displaying phosphatidylserine and the APC expressing TAM receptors (84, 117, 118). Phosphatidylserine also stabilizes the interaction between the TAM receptor and its ligands, preventing dissociation and ensuring strong and persistent down-stream intracellular signaling through the TAM receptor (84, 116-118). In this model, phosphatidylserine is the only immunosuppressive stimuli carried by an apoptotic cell (84), and the internalization or clearance of apoptotic bodies would not be absolutely required for tolerance induction.

The net result of TAM receptor signaling is inhibition of the same pro-inflammatory signaling pathways as GILZ, including NF-κB, MAPK and EKR-1/2 (84, 117-119). Specifically, signaling through Mer, a TAM receptor expressed on DCs, inhibits LPS-induced NF-κB activation and reduces IL-12 and TNF-α production (120, 121). Curiously both GILZ and TAM knockout mice have a similar phenotype in the testes, characterized by defects in the phagocytic clearance of apoptotic cells, a complete loss of the germ cell lineage, and male sterility (59, 84). Given the central importance of TAM receptors in clearing apoptotic bodies (84, 119), transmitting their immunosuppressive signals (120, 121), and inhibiting pro-inflammatory signaling

pathways after TLR-ligation (116, 117), the possibility that TAM receptor signaling leads to the downstream induction of GILZ should be further investigated.

An unanswered question from this study is whether interactions between apoptotic MoDCs and viable MoDCs may have been responsible for the induction of GILZ observed in PUVA-DC cultures. PUVA-DCs were cultured at low cell density and were relatively adherent to the plastic culture well. Nevertheless, the possibility remains that a small percentage of apoptotic MoDCs in culture may have generated membrane blebs with high levels of phosphatidylserine (111), capable of diffusing and bridging the distance between individual cells to transmit immunosuppressive signals.

Of note, the time course for GILZ induction differed greatly between Dex-DCs and PUVA-DCs (see **Figure 1E**). Dexamethasone induced maximum GILZ expression within 2 hr of PUVA treatment, and the expression remained elevated for at least 72 hr in culture. This observation is consistent with the known pharmacokinetics of glucocorticoids. Dexamethasone, like all glucocorticoids, is lipid soluble and rapidly diffuses into the cytoplasm of cells where it associates with the cytosolic glucocorticoid-receptor (70, 71). This complex then travels to the nucleus and binds to the glucocorticoid-response elements upstream of the GILZ promoter, thereby inducing GILZ mRNA transcription (70, 71). In contrast, PUVA-DCs did not demonstrate significant up-regulation of GILZ until 8 hr after PUVA treatment, and the maximum expression level occurred only after 24 hr. This suggests a fundamental difference between dexamethasone and PUVA treatment in regards to the mechanism leading to GILZ induction. The cellular events mediating the direct effects of PUVA on MoDCs, including the cellular stress response and DNA repair pathway activation, may take time

before GILZ mRNA is ultimately transcribed. Alternatively, this observation may be demonstrating that MoDCs must first enter the apoptotic pathway, and then be recognized and internalized by viable MoDCs, before the induction of GILZ occurs.

Nevertheless, GILZ was induced at high levels in MoDCs treated with PUVA doses that did not result in an increase in the percentage of early apoptotic MoDCs above the level observed in untreated cultures (see **Figure 2B**). However, if the immunosuppressive signals delivered by an apoptotic DC and an ApoL are not equivalent, then it may be possible for far fewer apoptotic DCs to mediate a tolerogenic effect. Indeed, there is evidence that there may be quantitative differences between various types of apoptotic cells. It is well known that mice with defects in apoptotic pathways mediated through Fas and FasL develop autoimmune disease (122). Specifically inhibiting DC apoptosis, but not lymphocyte apoptosis, leads to autoimmune disease, suggesting a unique role for DC apoptosis in the maintenance of tolerance (123). Moreover, when viable DCs internalize apoptotic, but not necrotic DCs, they become resistant to LPS maturation (124) and generate antigen-specific $Foxp3^{+}$ Tregs (124, 125). The induction of Tregs is a direct result of TGF-β1 secretion by viable DCs (122), previously shown to be necessary for the differentiation of naïve T-lymphocytes into Tregs (42, 43).

Macrophages also secrete TGF-β1 after ingesting apoptotic cells, and this TGF-β1 production is dependent on phosphatidylserine (126). Interestingly however, the internalization of apoptotic splenocytes by viable DCs does not induce TGF-β1 production (124, 125). Given that apoptotic splenocytes display phosphatidylserine, this observation suggests a phosphatidylserine-independent mechanism for TGF-β1 release

by viable DCs after internalization of apoptotic DCs, as well as the presence of key molecular differences between apoptotic DCs and non-DC apoptotic cells (122, 127). The unique receptors mediating TGF-β1 secretion after the uptake of apoptotic DCs are unknown, but may involve highly specific receptors, possibly αβ integrins, only expressed on the surface of apoptotic DCs (122, 127). The production of TGF-β mRNA transcripts in this present study were higher in PUVA-DCs than in untreated MoDCs exposed to ApoL (3.4-fold vs. 2.1-fold above untreated MoDCs, respectively), suggesting that the internalization of apoptotic MoDCs by viable MoDCs may have played a role in the induction of GILZ and transcription of TGF-β mRNA.

DCs expressing GILZ at high levels have been shown to generate antigen-specific Tregs, and GILZ, IL-10 and TGF-β are all necessary for this induction (42, 43, 69). Although this study did not specifically analyze Treg responses, MoDCs expressing GILZ increased production of IL-10 at both the protein and mRNA level, and increased TGF-β at the mRNA level. Given that an intravenous infusion of PUVA-treated apoptotic cells induces antigen-specific Tregs *in vivo* (31, 46, 47), it is reasonable that MoDCs expressing GILZ, and secreting IL-10 and TGF-β, would also be capable of inducing Tregs. Further studies will be needed to explore the possibility that MoDCs treated with PUVA, and/or exposed to ApoL, are capable of inducing Tregs in a similar fashion as Dex-DCs (69).

Both PUVA, and/or exposure to ApoL, induced GILZ expression to levels comparable with previous reports in human DCs (see **Figure 5B**) . Up-regulation of GILZ mRNA was confirmed by increased levels of GILZ protein, as assessed by intracellular flow cytometric analysis (see **Figure 5C**). However, the increase in GILZ

protein level did not follow the same trend as for GILZ mRNA up-regulation. This is most likely due to the fact that protein expression was only analyzed 24 hr after treatment, and the kinetics of both GILZ mRNA and protein up-regulation and stability varied depending on the specific type of treatment. Dex-DCs maximally up-regulated GILZ mRNA within 2 hr of treatment (see **Figure 1E**), and demonstrated the highest protein level after 24 hrs. In contrast, PUVA-DCs maximally up-regulated GILZ mRNA 24 hr after treatment, and therefore the protein level was found to be lower than that of Dex-DCs at the same time point. Lastly, MoDCs exposed to ApoL would be expected to have the slowest induction of GILZ mRNA and protein, given the requirement for phosphatidylserine exposure on lymphocytes, followed by recognition and processing by MoDCs. This may help explain why after 24 hr the GILZ mRNA levels were highest in MoDCs exposed to ApoL, but the proteins levels did not yet reflect this elevated mRNA expression. It would be useful to assess GILZ protein induction at earlier and later time points to more definitively clarify the kinetics of protein induction.

In addition, MoDCs expressing high levels of GILZ produced more IL-10 (see **Figure 6A**), and produced lesser amounts of various pro-inflammatory cytokines, including IL-12, IL-6, TNF-α, and IFN-γ (see **Figure 6B, 6C**). GILZ was necessary for the conversion to a tolerogenic cytokine profile, as evidenced by a reduction in IL-10 production, and an increase in IL-12p70 production, following transient siRNA-mediated GILZ knockdown (see **Figure 7B, 7C**). IL-12, IL-6, TNF-α, and IFN-γ are all inflammatory mediators released by immunogenic MoDCs in response to TLR ligation (34, 35). These cytokines polarize the immune response towards an inflammatory state, and help differentiate effector T-lymphocyte subsets and support their functions (34, 35).

MoDCs expressing high levels of GILZ also produced lesser amounts of various pro-inflammatory chemokines, including IL-8, MCP-1 (CCL2), MIP-1β (CCL4), and RANTES (CCL5) (see **Figure 6D, 6E**). These data support an earlier study in a monocytic cell line (THP-1), showing that GILZ expression reduced the production of both MIP-1α (CCL3) and RANTES (CCL5) (62). These chemokines are also produced by immunogenic MoDCs in response to TLR ligation, and they function as chemotactic factors, recruiting immune cells such as neutrophils, natural killer cells and T-lymphocytes to sites of inflammation or infection (34, 35).

This dualistic pattern of cytokine release, with reduced production of pro-inflammatory cytokines and increased production of anti-inflammatory cytokines, is central to UVB-induced, PUVA-induced, and ECP-induced immunomodulation (1). UVB induces IL-10 release from keratinocytes (128), and PUVA has been shown to significantly reduce the production of IL-6, IL-8, IL-1β and TNF-α (129). Likewise, in patients with chronic GVHD, ECP increases production of IL-10 (21, 51, 52) and IL-1Ra (21, 51, 52), and DCs cultured post-ECP produce no detectable levels of IL-1, IL-6 or IL-12 (21). While the general trend for reduced pro-inflammatory molecule production held true for all MoDCs demonstrating significant GILZ up-regulation, some groups did not achieve statistically significant reductions for individual cytokines and chemokines. This was most likely due to biological variability between individuals, and given a larger sample size, all groups would have likely achieved statistically significant reductions for all cytokines and chemokines. Lastly, PUVA could theoretically have globally suppressed the production of all pro-inflammatory molecules, however this is highly

unlikely given increased IL-10 production in the same MoDCs displaying reduced pro-inflammatory molecule production.

5.5. Implications for Extracorporeal Photochemotherapy

The results presented in this *in vitro* model of ECP have potentially important implications for the *in vivo* mechanisms operating after ECP. The vast majority of ECP-treated cells travel to either the spleen or liver following intravenous infusion (81). Splenic marginal zone DCs ingest circulating apoptotic cells as soon as 1 hr after intravenous injection (130), and in a different report, the highest percentage of splenic immature DCs with internalized apoptotic cells was detected 18 hr after injection (31). Although the mechanisms directing ECP-treated cells towards these anatomical locations are not known, the marginal zone of the spleen, in particular, contains abundant APCs capable of interacting with T-lymphocytes circulating through the spleen (81). It is conceivable that reinfusion of ECP-treated ApoL, and subsequent *in vivo* interactions with untreated tissue-resident splenic DCs, may induce GILZ expression and generate tolerogenic DCs capable of mediating antigen-specific immunosuppression. This would be analogous to the *in vivo* induction of GILZ within tissue-resident DCs after systemic glucocorticoid administration (59). It also points toward the marginal zone of the spleen as being the central anatomical location for tolerance induction elicited by ECP-treated apoptotic cells. Moreover, the liver has been broadly implicated as an anatomically important site for tolerance induction (110, 131), as antigen-triggered apoptosis results in the elimination of lymphoid cells by the liver (132).

In addition, the ECP procedure itself, through a combination of leukapheresis, flow dynamics on the plastic exposure plate, and interactions with platelets or other serum proteins, induces monocyte-to-DC differentiation (29). It is plausible that the effects of PUVA revealed by our *in vitro* study initiate a chain of events culminating in GILZ induction and the modulation of differentiating MoDCs. Interestingly, PUVA-DCs exposed to ApoL up-regulated GILZ to higher levels than either untreated MoDCs exposed to ApoL, or PUVA-DCs alone, suggesting a synergistic effect between PUVA treatment and ApoL exposure (see **Figure 5B**). It is tempting to speculate that PUVA may pre-condition MoDCs for the subsequent processing of ApoL, possibly by increasing the phagocytic capacity of differentiating MoDCs by up-regulating thrombospondin receptors (CD36) (133), TAM receptors, or other scavenger receptors. Given the synergism observed between PUVA-DCs and exposure to ApoL in regards to GILZ induction, MoDCs produced during the ECP procedure may also be uniquely pre-conditioned by PUVA treatment to generate tolerogenic immune responses *in vivo*.

In clinical use, patients' PBMC are exposed to UVA light as they pass extracorporeally through a thin exposure plate (7). While the centrifugation process to isolate PBMC from other cell types is quite efficient, there are still contaminating red blood cells flowing through the exposure plate that are capable of absorbing UVA radiation. Moreover, assuming laminar flow, cells in the center of the plate will flow faster than cells on the periphery. As a result of the plate's small, but non-zero thickness, laminar flow mechanics, and red cell contamination, it is possible that populations of monocytes, DCs, and differentiating MoDCs may be exposed to different amounts of UVA radiation from a fixed UVA light source. Therefore, sub-populations of APCs may

be modulated in subtle ways during the procedure, and may have different *in vivo* effects after reinfusion. Extrapolating from the data presented in this study, if a MoDC received a slightly smaller amount of UVA light energy, it may induce GILZ expression and be polarized towards the tolerogenic pathway. If a second MoDC received slightly more UVA light energy, it may enter the apoptotic pathway after reinfusion into the patient. The net result would be a complex interaction of cells *in vivo*, where MoDCs modulated to varying degrees would be mediating the final clinical response.

Two recent studies highlight the pivotal role for DCs in mediating *in vivo* tolerogenic responses after ECP. Firstly, Divito *et al.* challenged the conventional view that tolerogenic DCs suppress allograft rejection by interacting directly with anti-donor T-lymphocytes *in vivo* (134). This group demonstrated that an infusion of tolerogenic DCs prolonged heart allograft survival not by directly interacting with T-lymphocytes *in vivo*, but by being re-processed by recipient DCs (134) . The authors suggest that infusions of DCs are short-lived *in vivo*, and act as antigen-transporting cells, rather than APCs, to prolong allograft survival (134). This model supports the hypothesis that GILZ induction within tissue-resident DCs may be the initial event leading to tolerogenic responses observed after reinfusion of ECP-treated cells. Furthermore, it lends credence to the possibility that a small percentage of ECP-treated MoDCs undergoing early apoptosis are transmitting distinct tolerogenic signals (122-125) leading to GILZ up-regulation, and that the immunosuppressive signals are not transmitted solely by ApoL.

Secondly, a murine model of contact hypersensitivity demonstrated that the cell-mediated inhibition of a hapten immune response was lost when PUVA-treated splenocytes and lymph node cells from dinitrofluorobenzene (DNFB)-sensitized donors

were depleted of $CD11c^+$ DCs prior to their adoptive transfer into naïve mice (31). The tolerance was antigen-specific, as the naïve recipient mice retained the ability to properly respond to an unrelated hapten (31). Strikingly, there was still cell-mediated and antigen-specific inhibition of the same hapten immune response when PUVA-treated splenocytes and lymph node cells from DNFB-sensitized donors were instead depleted of $CD3^+$ lymphocytes (31). This implies, in this hapten model, that PUVA-treated $CD11c^+$ DCs are the primary and relevant cellular target for ECP in mediating tolerogenic responses *in vivo*.

Furthermore, the adoptive transfer of cells from primary recipients that had received ECP-treated cells significantly suppressed the DNFB response in secondary recipients, but the transfer capability was lost when the cells were depleted of $CD4^+$ or $CD25^+$ populations (31). Taken together, these results demonstrate that not only are the $CD11c^+$ DCs the primary cellular target of ECP, but they induce antigen-specific $CD4^+CD25^+$ Tregs *in vivo* (31). The hapten model does have the limitation that the antigen must be physically linked to the apoptotic cell, and only APCs retain this capacity for a long enough time *in vivo* to transmit meaningful tolerogenic signals (31). In other, non-haptenated models, ECP-treated APCs may not be as critical for the induction of tolerance, as has been demonstrated with other *in vivo* models of ECP (45-47).

Returning to the fundamental mystery surrounding ECP's clinical efficacy in CTCL (7), GVHD (8), allograft rejection (9), and autoimmune disease (10), it is worthwhile to consider how differences in immune responses may result from the intrinsic properties of patients' circulating lymphocytes. Varying percentages of malignant lymphocytes (known as Sézary cells) are present within peripheral blood in

patients with CTCL (135). This percentage can be particularly high if the patient has the leukemic variant of CTCL, known as Sézary syndrome (135, 136). Sézary cells are fundamentally abnormal. They possess numerous genetic mutations, gene deletions, and chromosomal translocations (137). They also have abnormal apoptotic pathways (138-140), and are insensitive to many traditional T-lymphocyte mitogens (141). In contrast, patients with GVHD, allograft rejection, and autoimmune disease, all have numerous benign, auto-reactive circulating lymphocytes. These are fundamentally normal lymphocytes performing their specialized functions, albeit they are targeting self-tissues or allogeneic grafts and inflicting tissue damage in the process. As such, it is not unreasonable to speculate that the responses of malignant Sézary cells and benign auto-reactive lymphocytes to ECP may be vastly different, and translate into distinct immune responses.

The kinetics of apoptotic induction, and the activation state of the apoptotic cell, both play a key role in influencing the immunogenicity or tolerogenicity of the apoptotic stimulus (110). Given their numerous genetic and apoptotic pathway abnormalities (137-140), Sézary cells may rapidly undergo apoptosis in large numbers after ECP, effectively outstripping the phagocytic capacity of DCs to ingest and process them. Sézary cells would then become secondarily necrotic and release numerous DAMPs and immunogenic factors (115). Upon reinfusion into the patient, apoptotic Sézary cells, in combination with these pro-inflammatory mediators, would polarize an immunogenic T_h1 and cytotoxic T-lymphocyte immune response to target and eradicate the malignant cells (136). Alternatively, given aberrant apoptotic pathways, Sézary cells may not possess the capacity to oxidize HMGB-1 in a caspase-dependent fashion, resulting in an overly

immunogenic apoptotic cell (115). It has also been shown that anti-CD3-activated T-lymphocytes express CD154, which converts a normally tolerogenic apoptotic lymphocyte into an immunogenic stimulus (142). Interestingly, Sézary cells express many activation markers, including CD45RO (135), CD25 (135), and STAT3 (143), and the malignant cells' persistent state of activation may play a role in the pathogenesis of CTCL (135). In summary, the rapid and wide-spread induction of apoptosis, release of DAMPs, and the persistent activation state of Sézary cells, may all play a role in polarizing an immunogenic response after ECP in patients with CTCL.

On the other hand, auto-reactive T-lymphocytes may undergo a controlled, slower apoptotic cell death after ECP, producing immunosuppressive membrane blebs (111) that are efficiently cleared by DCs before becoming secondarily necrotic and releasing DAMPs. The net *in vivo* effect would be the induction of GILZ within tissue-resident DCs, possibly in the spleen or liver, the subsequent generation of tolerogenic DCs, and the induction of antigen-specific immune tolerance through Treg generation. Investigating the differing susceptibilities of Sézary cells from CTCL patients, and auto-reactive lymphocytes from GVHD patients, including the kinetics of cell death following ECP and the release of pro-inflammatory mediators, may shed light on this central unanswered question regarding the immunodulation observed after ECP.

5.6. Concluding Remarks

In conclusion, PUVA acts directly, and indirectly via the generation of ApoL, to induce GILZ expression and polarize MoDCs towards a tolerogenic phenotype and functional state. MoDCs expressing GILZ are characterized phenotypically by reduced

expression of co-stimulatory molecules and resistance to full maturation by LPS. MoDCs expressing GILZ are characterized functionally by increased production of immunosuppressive cytokines, and reduced production of pro-inflammatory cytokines and chemokines. GILZ is necessary for the PUVA-mediated generation of this tolerogenic cytokine profile in MoDCs, as IL-10 production was decreased and IL-12 production was increased following transient siRNA-mediated knockdown of GILZ.

This study provides a molecular explanation for the immunosuppressive signals delivered by PUVA and apoptotic cells, and contributes towards explaining how ECP can generate antigen-specific immunosuppression. It also links PUVA and apoptotic cells with glucocorticoids, IL-10 and TGF-β. All share a common mechanism for immune regulation at the level of GILZ induction and inhibition of NF-κB and other pro-inflammatory signaling pathways. The critical difference between ECP and glucocorticoid therapy lies in the steroid-sparing action of both PUVA and apoptotic cells. ECP induces antigen-specific immunomodulation, thereby protecting the patient from the side effects of chronic steroid therapy, including an increased rate of infection and malignancy, adverse metabolic effects, and detrimental effects on bone and endocrine health (70, 71).

It will be important to determine whether the two PUVA-mediated methods of GILZ induction that we have identified can form the basis for novel therapeutic design. If the answer is affirmative, then over 20 years of clinical experience with ECP will be a lucrative source for these derived advances. ECP could form the basis for strategies aimed at selectively inducing GILZ expression in DCs, representing a promising

therapeutic avenue to promote the induction and maintenance of tolerance in GVHD, allograft rejection, and autoimmune diseases (144).

Furthermore, DC vaccines are capable of generating proficient anti-tumor responses *in vitro*, but have failed to produce durable clinical responses. A principle reason for this universal shortcoming is the inhibitory microenvironment established by tumors that provides a powerful, suppressive influence on the anti-tumor immune response (145). A recent study even revealed that the tumor microenvironment induced GILZ expression within DCs found at the site of tumors, thereby suppressing their anti-tumor immunogenic activity (145). Interestingly, blocking GILZ within DC vaccines prolonged the survival of mice with a pre-existing tolerogenic tumor microenvironment (145). This study suggests that selectively blocking GILZ activation may represent a novel strategy to translate the *in vitro* anti-tumor responses observed with DC vaccines into durable *in vivo* clinical responses. Continued investigation into the mechanism of ECP may shed light on how to modify and enhance the therapy to selectively activate GILZ in diseases of auto-reactive lymphocytes, and turn off GILZ in the design of DC vaccines for solid-tumor immunotherapy.

From reports of the ancient Egyptians using the *Ammi majus* plant growing alongside the Nile River to treat skin disease, to the characterization of its active component as a psoralen, UVA radiation combined with photosensitizing psoralens has remained an effective dermatologic therapy. ECP has the potential to polarize DCs towards a tolerogenic or immunogenic pathway by simply switching GILZ on or off depending on which type of immunomodulation is desired for a given disease. It is remarkably appealing to consider the simplicity of using a small molecule and UV

radiation to selectively stimulate the immune response to target cancer in CTCL, malignant melanoma, and other solid-organ tumors, and selectively suppress the immune response in GVHD, solid-organ transplant rejection, and autoimmune disease.

References

1. Dupont, E., and Craciun, L. 2009. UV-induced immunosuppressive and anti-inflammatory and anti-inflammatory actions: mechanisms and clinical applications. *Immunotherapy.* 1:205-210.
2. Kripke, M. 1974. Antigenicity of murine skin tumors induced by ultraviolet light. *J. Natl. Cancer. Inst.* 53:1333-1336.
3. Aubin, F., and Mousson, C. 2004. Ultraviolet light-induced regulatory (suppressor) T cells: an approach for promoting induction of operational allograft tolerance? *Transplantation.* 77:S29-31.
4. Greene, M.I., Sy, M.S., Kripke, M., and Benacerraf, B. 1979. Impairment of antigen-presenting cell function by ultraviolet radiation. *Proc. Natl. Acad. Sci. USA.* 76:6591-6595.
5. Toews, G.B., Bergstresser, P.R., and Streilein, J.W. 1980. Epidermal Langerhans cell density determines whether contact hypersensitivity or unresponsiveness follows skin painting with DNFB. *J. Immunol.* 124:445-453.
6. Parrish, J.A., Fitzpatrick, T.B., Tanenbaum, L., and Pathak, M.A. 1974. Photochemotherapy of psoriasis with oral methoxsalen and longwave ultraviolet light. *N. Engl. J. Med.* 291:1207-1211.
7. Edelson, R., Berger, C., Gasparro, F., Jegasothy, B., Heald, P., *et al.* 1987. Treatment of cutaneous T-cell lymphoma by extracorporeal photochemotherapy. Preliminary results. *N. Engl. J. Med.* 316:297-303.
8. Greinix, H.T., Volc-Platzer, B., Rabitsch, W., Gmeinhart, B., Guevara-Pineda, C., *et al.* 1998. Successful use of extracorporeal photochemotherapy in the treatment of severe acute and chronic graft-versus-host disease. *Blood.* 92:3098-3104.
9. Wieland, M., Thieda, V.L., Strauss, R.G., Piette, W.W., Kapelanski, D.P., *et al*. 1994. Treatment of severe cardiac allograft rejection with extracorporeal photochemotherapy. *J. Clin. Apher.* 9:171-175.
10. Knobler, R., Barr, M. L., Couriel, D. R., Ferrara, J. L., French, L. E., *et al*. 2009. Extracorporeal photopheresis: past, present, and future. *J. Am. Acad. Dermatol.* 61:652-665.
11. Lai, C., Cao, H., Hearst, J.E., Corash, L., Luo, H., and Wang, Y. 2008. Quantitative Analysis of DNA Interstrand Cross-Links and Monoadducts Formed in Human Cells Induced by Psoralens and UVA Irradiation. *Anal. Chem.* 80:8790-8798.
12. Tambur, A., Ortegel, J., Morales, A., Klingemann, H., Gebel, H.M., *et al*. 2000. Extracorporeal photopheresis induces lymphocyte but not monocyte apoptosis. *Transplant. Proc.* 32:747-748.
13. Yoo, E.K., Rook, A.H., Elenitsas, R., Gasparro, F.P., and Vowels, B.R. 1996. Apoptosis induction by ultraviolet light A and photochemotherapy in cutaneous T-cell lymphoma: relevance to mechanism of therapeutic action. *J. Invest. Dermatol.* 107:235-242.
14. Wolnicka-Glubisz, A., Fraczek, J., Skrzeczynska-Moncznik, J., Friedlein, G., Mikolajczyk, T., *et al.* 2010. Effect of UVA and 8-methoxypsoralen, 4, 6, 4'-trimethylangelicin or chlorpromazine on apoptosis of lymphocytes and their recognition by monocytes. *J. Physiol. Pharmacol.* 61:107-114.

15. Viola, G., Fortunato, E., Cecconet, L., Disaro, S., and Basso, G. 2007. Induction of apoptosis in Jurkat cells by photoexcited psoralen derivatives: Implication of mitochondrial dysfunctions and caspases activation. *Toxicol. In Vitro.* 21:211-216.
16. Godar, D.E. 1999. UVA1 radiation triggers two different final apoptotic pathways. *J. Invest. Dermatol.* 112:3-12.
17. Bladon, J., and Taylor, P.C. 2002. Extracorporeal photopheresis in cutaneous T-cell lymphoma and graft-versus-host disease induces both immediate and progressive apoptotic processes. *Br. J. Dermatol.* 146:59-68.
18. Di Renzo, M., Rubegni, P., Sbano, P., Cuccia, A., Castagnini, C., *et al*. 2003. ECP-treated lymphocytes of chronic graft-versus-host disease patients undergo apoptosis which involves both the Fas/FasL system and the Bcl-2 protein family. *Arch. Dermatol. Res.* 295:175-182.
19. Lischka, G. 1979. Lymphocyte proliferation during PUVA therapy. *Arch. Dermatol. Res.* 264:213-218.
20. Berger, C.L., Cantor, C., Wellsh, J., Dervan, P., Begley, T., *et al*. 1985. Comparison of synthetic psoralen derivatives and 8-MOP in the inhibition of lymphocyte proliferation. *Ann. N.Y. Acad. Sci.* 453:80-90.
21. Spisek, R., Gasova, Z., and Bartunkova, J. 2006. Maturation state of dendritic cells during the extracorporeal photopheresis and its relevance for the treatment of chronic graft-versus-host disease. *Transfusion.* 46:55-65.
22. Merrick, A., Errington, F., Milward, K., O'Donnell, D., Harrington, K., *et al*. 2005. Immunosuppressive effects of radiation on human dendritic cells: reduced IL-12 production on activation and impairment of naive T-cell priming. *Br. J. Cancer.* 92:1450-1458.
23. Di Renzo, M., Rubegni, P., Pasqui, A. L., Pompella, G., De Aloe, G., *et al.* 2005. Extracorporeal photopheresis affects interleukin (IL)-10 and IL-12 production by monocytes in patients with chronic graft-versus-host disease. *Br. J. Dermatol.* 153:59-65.
24. Lamioni, A., Parisi, F., Isacchi, G., Giorda, E., and Di Cesare, S. 2005. The Immunological Effects of Extracorporeal Photopheresis Unraveled: Induction of Tolerogenic Dendritic Cells In Vitro and Regulatory T Cells In Vivo. *Transplantation.* 79:846-850.
25. Holtick, U., Marshall, S.R., Wang, X.N., Hilkens, C.M., and Dickinson, A.M. 2008. Impact of psoralen/UVA-treatment on survival, activation, and immunostimulatory capacity of monocyte-derived dendritic cells. *Transplantation.* 85:757-766.
26. Rao, V., Saunes, M., Jorstad, S., and Moen, T. 2008. In vitro experiments demonstrate that monocytes and dendritic cells are rendered apoptotic by extracorporeal photochemotherapy, but exhibit unaffected surviving and maturing capacity after 30 Gy gamma irradiation. *Scand. J. Immunol.* 68:645-651.
27. Edelson, R.L. 2001. Cutaneous T cell lymphoma: the helping hand of dendritic cells. *Ann. N.Y. Acad. Sci.* 941:1-11.
28. Szodoray, P., Papp, G., Nakken, B., Harangi, M., and Zeher, M. 2010. The molecular and clinical rationale of extracorporeal photochemotherapy in

autoimmune diseases, malignancies and transplantation. *Autoimmun. Rev.* 9:459-464.
29. Berger, C., Hoffmann, K., Vasquez, J.G., Mane, S., and Lewis, J. 2010. Rapid generation of maturationally synchronized human dendritic cells: contribution to the clinical efficacy of extracorporeal photochemotherapy. *Blood.* 116:4838-4847.
30. Plumas, J., Manches, O., and Chaperot, L. 2003. Mechanisms of action of extracorporeal photochemotherapy in the control of GVHD: involvement of dendritic cells. *Leukemia.* 17:2061-2062.
31. Maeda, A., Schwarz, A., Kernebeck, K., Gross, N., and Aragane, Y. 2005. Intravenous infusion of syngeneic apoptotic cells by photopheresis induces antigen-specific regulatory T cells. *J. Immunol.* 174:5968-5976.
32. Bladon, J., and Taylor, P.C. 2006. Extracorporeal photopheresis: a focus on apoptosis and cytokines. *J. Dermatol. Sci.* 43:85-94.
33. Tokura, Y., Seo, N., Yagi, H., and Takigawa, M. 2001. Photoactivational cytokine-modulatory action of 8-methoxypsoralen plus ultraviolet A in lymphocytes, monocytes and cutaneous T cell lymphoma cells. *Ann. N.Y. Acad. Sci.* 941:185-193.
34. Steinman, R.M. 1991. The dendritic cell system and its role in immunogenicity. *Annu. Rev. Immunol.* 9:271-296.
35. Banchereau, J., Briere, F., Caux, C., Davoust, J., and Lebecque, S. 2000. Immunobiology of dendritic cells. *Annu. Rev. Immunol.* 18:767-811.
36. Steinman, R.M., Hawiger, D., and Nussenzweig, M.C. 2003. Tolerogenic dendritic cells. *Annu. Rev. Immunol.* 21:685-711.
37. e Sousa, C.R. 2006. Dendritic cells in a mature age. *Nat. Rev. Immunol.* 6:476-483.
38. Lutz, M.B., and Schuler, G. 2002. Immature, semi-mature and fully mature dendritic cells: which signals induce tolerance or immunity? *Trends Immunol.* 23:445-449.
39. Zanomi, I., Ostuni, G., Capuano, M., Collini, M., Caccia, M., *et al*. 2009. CD14 regulates the dendritic cell life cycle after LPS exposure through NFAT activation. *Nature.* 460:264-268.
40. Hu, J., and Wan, Y. 2011. Tolerogenic dendritic cells and their potential applications. *Immunology.* 132:307-314.
41. Manicassamy, S., and Pulendran, B. 2011. Dendritic cell control of tolerogenic responses. *Immunol. Rev.* 241:206-227.
42. Morel, P.A., and Turner, M.S. 2011. Dendritic cells and the maintenance of self-tolerance. *Immunol. Res.* 50:124-129.
43. Maldonado, R.A., and von Andrian, U.H. 2010. How tolerogenic dendritic cells induce regulatory T cells. *Adv. Immunol.* 108:111-165.
44. Hadeiba, H., Sato, T., Habtezion, A., Oderup, C., Pan, J., and Butcher, E.C. 2008. CCR9 expression defines tolerogenic plasmacytoid dendritic cells able to suppress acute graft-versus-host disease. *Nat. Immunol.* 9:1253-1260.
45. Gatza, E., Rogers, C.E., Clouthier, S.G., Lowler, K.P., and Tawara, I. 2008. Extracorporeal photopheresis reverses experimental graft-versus-host disease through regulatory T cells. *Blood.* 112:1515-1521.

46. Zheng, D.H., Dou, L.P., Wei, Y.X., Du, G.S., and Zou, Y.P. 2010. Uptake of donor lymphocytes treated with 8-methoxypsoralen and ultraviolet A light by recipient dendritic cells induces CD4+CD25+Foxp3+ regulatory T cells and down-regulates cardiac allograft rejection. *Biochem. Biophys. Res. Commun.* 395:540-546.
47. Wang, Z., Larregina, A.T., Shufesky, W.J., Perone, M.J., and Montecalvo, A. 2006. Use of the inhibitory effect of apoptotic cells on dendritic cells for graft survival via T-cell deletion and regulatory T cells. *Am. J. Transplant.* 6:1297-1311.
48. Maeda, A., Schwarz, A., Bullinger, A., Morita, A., Peritt, D., and Schwarz, T. 2008. Experimental extracorporeal photopheresis inhibits the sensitization and effector phases of contact hypersensitivity via two mechanisms: generation of IL-10 and induction of regulatory T cells. *J. Immunol.* 181:5956-5962.
49. Biagi, E., Di Biaso, I., Leoni, V., Gaipa, G., and Rossi, V. 2007. Extracorporeal photochemotherapy is accompanied by increasing levels of circulating CD4+CD25+GITR+Foxp3+CD62L+ functional regulatory T-cells in patients with graft-versus-host disease. *Transplantation.* 84:31-39.
50. Suchin, K.R., Cassin, M., Washko, R., Nahass, G., Berkson, M., *et al*. 1999. Extracorporeal photochemotherapy does not suppress T-or B-cell responses to novel or recall antigens. *J. Am. Acad. Dermatol.* 41:980-986.
51. Craciun, L.I.D., M., Schandene, L., Laub, R., Goldman, M., and Dupont, E. 2005. Anti-inflammatory effects of UV-irradiated lymphocytes: induction of IL-1Ra upon phagocytosis by monocyte/macrophages. *Clin. Immunol.* 114:320-326.
52. Craciun, L.I., Stordeur, P., Schandene, L., Duvillier, H., Bron, D., *et al*. 2002. Increased production of interleukin-10 and interleukin-1 receptor antagonist after extracorporeal photochemotherapy in chronic graft-versus-host disease. *Transplantation.* 74:995-1000.
53. Legitimo, A., Consolini, R., Failli, A., Fabiano, S., Bencivelli, W., *et al*. 2007. In vitro treatment of monocytes with 8-methoxypsolaren and ultraviolet A light induces dendritic cells with a tolerogenic phenotype. *Clin. Exp. Immunol.* 148:564-572.
54. Gorgun, G., Miller, K.B., and Foss, F.M. 2002. Immunologic mechanisms of extracorporeal photochemotherapy in chronic graft-versus-host disease. *Blood.* 100:941-947.
55. Moser, M., De Smedt, T., Sornasse, T., Tielemans, F., Chentoufi, A.A., *et al*. 1995. Glucocorticoids down-regulate dendritic cell function in vitro and in vivo. *Eur. J. Immunol.* 25:2818-2824.
56. Piemonti, L., Monti, P., Allavena, P., Leone, B.E., Caputa, A., and Di Carlo, V. 1999. Glucocorticoids increase the endocytic capacity of human dendritic cells. *Int. Immunol.* 11:1519-1526.
57. Rea, D., van Kooten, C., van Maijgaarden K.E., Ottenhoff, T.H., Melief, C.J., and Offringa, R. 2000. Glucocorticoids transform CD40-triggering of dendritic cells into an alternative activation pathway resulting in antigen-presenting cells that secrete IL-10. *Blood.* 95:3162-3167.

58. Unger, W.W., Laban, S., Kleijwegt, F.S., van der Slik, A.R., and Roep, B.O. 2009. Induction of Treg by monocyte-derived DC modulated by vitamin D3 or dexamethasone: differential role for PD-L1. *Eur. J. Immunol.* 39:3147-3159.
59. Cohen, N., Mouly, E., Hamdi, H., Maillot, M.C., and Pallardy, M. 2006. GILZ expression in human dendritic cells redirects their maturation and prevents antigen-specific T lymphocyte response. *Blood.* 107:2037-2044.
60. D'Adamio, F., Zollo, O., Moraca, R., Ayroldi, E., Bruscoli, S., *et al*. 1997. A new dexamethasone-induced gene of the leucine zipper family protects T lymphocytes from TCR/CD3-activated cell death. *Immunity.* 7:803-812.
61. Ayroldi, E., Zollo, O., Macchiarulo, A., Di Marco, B., Marchetti, C., and Riccardi, C. 2002. Glucocorticoid-Induced Leucine Zipper Inhibits the Raf-Extracellular Signal-Regulated Kinase Pathway by Binding to Raf-1. *Mol. Cell. Biol.* 22:7929-7941.
62. Berrebi, D., Bruscoli, S., Cohen, N., Foussat, A., Migliorati, G., *et al*. 2003. . Synthesis of glucocorticoid-induced leucine zipper (GILZ) by macrophages: an anti-inflammatory and immunosuppressive mechanism shared by glucocorticoids and IL-10. *Blood.* 101:729-738.
63. Godot, V., Garcia, G., Capel, F., Arock, M., Durand-Gasselin, I., *et al*. 2006. Dexamethasone and IL-10 stimulate glucocorticoid-induced leucine zipper synthesis by human mast cells. *Allergy.* 61:886-890.
64. He, L., Yang, N., Isales, C.M., and Shi, X.M. 2012. Glucocorticoid-induced leucine zipper (GILZ) antagonizes TNF-alpha inhibition of mesenchymal stem cell osteogenic differentiation. *PLoS One.* 7:e31717.
65. Soundararajan, R., Zhang, T.T., Wang, J., Vandewalle, A., and Pearce, D. 2005. A novel role for glucocorticoid-induced leucine zipper protein in epithelial sodium channel-mediated sodium transport. *J. Biol. Chem.* 280:39970-39981.
66. Eddleston, J., Herschbach, J., Wagelie-Steffen, A.L., Christiansen, S.C., and Zuraw, B.L. 2007. The anti-inflammatory effect of glucocorticoids is mediated by glucocorticoid-induced leucine zipper in epithelial cells. *J. Allergy Clin. Immunol.* 119:115-122.
67. Bruscoli, S., Velardi, E., Di Sante, M., Bereshchenko, O., Venanzi, A., *et al*. 2012. Long glucocorticoid-induced leucine zipper (L-GILZ) protein interacts with ras protein pathway and contributes to spermatogenesis control. *J. Biol. Chem.* 287:1242-1251.
68. Ellestad, L.E., Malkiewicz, S.A., Guthrie, H.D., Welch, G.R., and Porter, T.E. 2009. Expression and regulation of glucocorticoid-induced leucine zipper in the developing anterior pituitary gland. *J. Mol. Endocrinol.* 42:171-183.
69. Hamdi, H., Godot, V., Maillot, M.C., Prejean, M.V., and Cohen, N. 2007. Induction of antigen-specific regulatory T lymphocytes by human dendritic cells expressing the glucocorticoid-induced leucine zipper. *Blood.* 110:211-219.
70. Beaulieu, E., and Morand, E.F. 2011. Role of GILZ in immune regulation, glucocorticoid actions and rheumatoid arthritis. *Nat. Rev. Rheumatol.* 7:340-348.
71. Baschant, U., and Tuckermann, J. 2010. The role of the glucocorticoid receptor in inflammation and immunity. *J. Steroid Biochem. Mol. Biol.* 120:69-75.
72. Di Marco, B., Massetti, M.. Bruscoli, S., Macchiarulo, A., Di Virgilio, R., *et al*. 2007. Glucocorticoid-induced leucine zipper (GILZ)/NF-kappaB interaction: role

of GILZ homo-dimerization and C-terminal domain. *Nucleic Acids Res.* 35:517-528.
73. Corinti, S., Albanesi, C., la Sala, A., Pastore, S., and Girolomoni, G. 2001. Regulatory activity of autocrine IL-10 on dendritic cell functions. *J. Immunol.* 166:4312-4318.
74. Voll, R.E., Herrmann, M., Roth, E.A., Stach, C., J.R., K., and Girkontaite, I. 1997. Immunosuppressive effects of apoptotic cells. *Nature.* 390:350-351.
75. Byrne, A., and Reen, D.J. 2002. Lipopolysaccharide induces rapid production of IL-10 by monocytes in the presence of apoptotic neutrophils. *J. Immunol.* 168:1968-1976.
76. Fadok, V.A., Bratton, D.L., Konowal, A., Freed, P.W., Westcott, J.Y., and Henson, P.M. 1998. Macrophages that have ingested apoptotic cells in vitro inhibit proinflammatory cytokine production through autocrine/paracrine mechanisms involving TGF-beta, PGE2, and PAF. *J. Clin. Invest.* 101:890-898.
77. Sauter, B., Albert, M.L., Francisco, L., Larsson, M., Somersan, S., and Bhardwaj, N. 2000. Consequences of cell death: exposure to necrotic tumor cells, but not primary tissue cells or apoptotic cells, induces the maturation of immunostimulatory dendritic cells. *J. Exp. Med.* 191:423-434.
78. Albert, M.L., Pearce, S.F., Francisco, L.M., Sauter, B., Roy, P., *et al*. 1998. Immature dendritic cells phagocytose apoptotic cells via alphavbeta5 and CD36, and cross-present antigens to cytotoxic T lymphocytes. *J. Exp. Med.* 188:1359-1368.
79. Stuart, L.M., Lucas, M., Simpson, C., Lamb, J., Savill, J., and Lacy-Hulbert, A. 2002. Inhibitory effects of apoptotic cell ingestion upon endotoxin-driven myeloid dendritic cell maturation. *J. Immunol.* 168:1627-1635.
80. Clayton, A.R., Prue, R.L., Harper, L., Drayson, M.T., and Savage, C.O. 2003. Dendritic cell uptake of human apoptotic and necrotic neutrophils inhibits CD40, CD80, and CD86 expression and reduces allogeneic T cell responses: relevance to systemic vasculitis. *Arthritis Rheum.* 48:2362-2374.
81. Xia, C.Q., Campbell K.A., and Clare-Salzler, M.J. 2009. Extracorporeal photopheresis-induced immune tolerance: a focus on modulation of antigen-presenting cells and induction of regulatory T cells by apoptotic cells. *Curr. Opin. Organ Transplant.* 14:338-343.
82. Fadok, V.A., Voelker, D.R., Campbell, P.A., Cohen, J.J., Bratton, D.L., and Henson, P.M. 1992. Exposure of phosphatidylserine on the surface of apoptotic lymphocytes triggers specific recognition and removal by macrophages. *J. Immunol.* 148:2207-2216.
83. Castedo, M., Hirsch, T., Susin, S.A., Zamzami, N., Marchetti, P., *et al*. 1996. Sequential acquisition of mitochondrial and plasma membrane alterations during early lymphocyte apoptosis. *J. Immunol.* 157:512-521.
84. Lemke, G., and Rothlin, C.V. 2008. Immunobiology of the TAM receptors. *Nat. Rev. Immunol.* 8:327-336.
85. Kim, S., Elkon, K.B., and Ma, X. 2004. Transcriptional suppression of interleukin-12 gene expression following phagocytosis of apoptotic cells. *Immunity.* 21:643-653.

86. Dauer, M., Obermaier, B., Herten, J., Haerle, C., and Pohl, K. 2003. Mature dendritic cells derived from human monocytes within 48 hours: a novel strategy for dendritic cell differentiation from blood precursors. *J. Immunol.* 170:4069-4076.
87. Kvistborg, P., Boegh, M., Pedersen, A.W., Claesson, M.H., and Zocca, M.B. 2009. Fast generation of dendritic cells. *Cell. Immunol.* 260:56-62.
88. Jarnjak-Jankovic, S., Hammerstad, H., Saeboe-Larssen, S., Kvalheim, G., and Gaudernack, G. 2007. A full scale comparative study of methods for generation of functional dendritic cells for use as cancer vaccines. *BMC Cancer.* 7:119-127.
89. Zhou, L.J., and Tedder, T.F. 1996. CD14+ blood monocytes can differentiate into functionally mature CD83+ dendritic cells. *Proc. Natl. Acad. Sci. USA*. 93:2588-2592.
90. Klein, E., Koch, S., Borm, B., Neumann, J., and Herzog, V. 2005. CD83 localization in a recycling compartment of immature human monocyte-derived dendritic cells. *Int. Immunol.* 17:477-487.
91. Gasparro, F.P., Bevilacqua, P.M., Goldminz, D., and Edelson, R. 1990. Repair of 8-MOP photoadducts in human lymphocytes. In *DNA Damage and Repair in Human Tissues* B.M. Sutherland, and Woodhead, A.D., editor. New York: Springer US. 137-148.
92. Piemonti, L., Monti, P., Allavena, P., Sironi, M., Soldini, L., *et al*. 1999. Glucocorticoids affect human dendritic cell differentiation and maturation. *J. Immunol.* 162:6473-6481.
93. Verhasselt, V., Buelens, C., Willems, F., De Groote, D., Haeffner-Cavaillon, N., and Goldman, M. 1997. Bacterial lipopolysaccharide stimulates the production of cytokines and the expression of costimulatory molecules by human peripheral blood dendritic cells: evidence for a soluble CD14-dependent pathway. *J. Immunol.* 158:2919-2925.
94. Stein, B., Rahmsdorf, H.J., Steffern, A., Litfin, M., and Herrlich, P. 1989. UV-induced DNA damage is an intermediate step in UV-induced expression of human immunodeficiency virus type 1, collagenase, c-fos, and metallothionein. *Mol. Cell. Biol.* 9:5169-5181.
95. Alge, C., Baxter, R.M., Doyle, M.E., Moor, A.C., Brissette, J.L., and Ortel, B. 2001. PUVA downregulates whn expression in primary mouse keratinocytes. *J. Photochem. Photobiol. B.* 64:75-81.
96. Bordin, F., Carlassare, F., Busulini, L. and Baccichetti, F. 1993. Furocoumarin sensitization induces DNA-protein cross-links. *Photochem. Photobiol.* 58:133-136.
97. Heck, D.E., Bisaccia, E., Armus, S., and Laskin, J.D. 1991. Production of hydrogen peroxide by cutaneous T-cell lymphoma following photopheresis with psoralens and ultraviolet light. *Cancer Chemother. Pharmacol.* 28:344-350.
98. Moor, A.C., Schmitt, I.M., Beijersbergen van Hengouwen, G.M., Chimenti, S., Edelson, R.L., and Gasparro, F.P. 1995. Treatment with 8-MOP and UVA enhances MHC class I synthesis in RMA cells: preliminary results. *J. Photochem. Photobiol. B.* 29:193-198.
99. Gasparro, F.P. 1996. Psoralen photobiology: recent advances. *Photochem. Photobiol.* 63:553-557.

100. Gasparro, F.P., Dall'Amico, R., Goldminz, D., Simmons, E., and Weingold, D. 1989. Molecular aspects of extracorporeal photochemotherapy. *Yale J. Biol. Med.* 62:579-593.
101. Asselin-Labat, M.L., David, M., Biola-Vidamment, A., Lecoeuche, D., and Zennaro, M.C. 2004. GILZ, a new target for the transcription factor FoxO3, protects T lymphocytes from interleukin-2 withdrawal-induced apoptosis. *Blood.* 104:215-223.
102. Wang, Y., Ma, Y.Y., Song, X.L., Cai, H.Y., and Chen, J.C. 2012. Upregulations of glucocorticoid-induced leucine zipper by hypoxia and glucocorticoid inhibit proinflammatory cytokines under hypoxic conditions in macrophages. *J. Immunol.* 188:222-229.
103. Delfino, D.V., Spinicelli, S., Pozzesi, N., Pierangeli, S., Velardi, E., *et al*. 2011. Glucocorticoid-induced activation of caspase-8 protects the glucocorticoid-induced protein Gilz from proteasomal degradation and induces its binding to SUMO-1 in murine thymocytes. *Cell Death Differ.* 18:183-190.
104. Spiering, R., van der Zee, R., Wagenaar, J., Kapetis, D., Zolezzi, F., *et al*. 2012. Tolerogenic dendritic cells that inhibit autoimmune arthritis can be induced by a combination of carvacrol and thermal stress. *PLoS One.* 7:e46336.
105. Gomez, M., Raju, S.V., Viswanathan, A., Painter, R. G., Bonvillain, R., *et al*. 2010. Ethanol upregulates glucocorticoid-induced leucine zipper expression and modulates cellular inflammatory responses in lung epithelial cells. *J. Immunol.* 184:5715-5722.
106. Koberle, M., Goppel, D., Grandl, T., Gaentzsch, P., Manncke, B., Berchtold, S., *et al*. 2012. Yersinia enterocolitica YopT and Clostridium difficile Toxin B induce expression of GILZ in epithelial cells. *PLoS One.* 7:e40730.
107. Yang, J., Bernier, S.M., Ichim, T.E., Li, M., and Xia, X. 2003. LF15-0195 generates tolerogenic dendritic cells by suppression of NF- B signaling through inhibition of IKK activity. *J. Leukoc. Biol.* 74:438-447.
108. Sen, P., Wallet, M.A., Yi, Z., Huang, Y., Henderson, M., *et al*. 2007. Apoptotic cells induce Mer tyrosine kinase-dependent blockade of NF-κB activation in dendritic cells. *Blood.* 109:653-660.
109. Steinman, R.M., Turley, S., Mellman, I., and Inaba, K. 2000. The induction of tolerance by dendritic cells that have captured apoptotic cells. *J. Exp. Med.* 191:411-416.
110. Griffith, T.S., and Ferguson, T.A. 2011. Cell death in the maintenance and abrogation of tolerance: the five ws of dying cells. *Immunity.* 35:456-466.
111. Stadler, K., Frey, B., Munoz, L. E., Finzel, S., Rech, J., *et al*. 2009. Photopheresis with UV-A light and 8-methoxypsoralen leads to cell death and to release of blebs with anti-inflammatory phenotype in activated and non-activated lymphocytes. *Biochem. Biophys. Res. Commun.* 386:71-76.
112. Gao, Y., Herndon, J.M., Zhang, H., Griffith, T.S., and Ferguson, T.A. 1998. Antiinflammatory effects of CD95 ligand (FasL)-induced apoptosis. *J. Exp. Med.* 188:887-896.
113. Chen, W., Frank, M.E., Jin, W., and Wahl, S.M. 2001. TGF-beta released by apoptotic T cells contributes to an immunosuppressive milieu. *Immunity.* 14:715-725.

114. Tomimori, Y., Ikawa, Y., and Oyaizu, N. 2000. Ultraviolet-irradiated apoptotic lymphocytes produce interleukin-10 by themselves. *Immunol. Lett.* 71:49-54.
115. Kazama, H., Ricci, J.E., Herndon, J.M., Hoppe, G., Green, D.R., and Ferguson, T.A. 2008. Induction of immunologic tolerance requires caspase-dependent oxidation of high-mobility group box-1 protein. *Immunity.* 29:21-32.
116. Rothlin, C.V., and Lemke, G. 2010. TAM receptor signaling and autoimmune disease. *Curr. Opin. Immunol.* 22:740-746.
117. Rothlin, C.V., Ghosh, S., Zuniga, E.I., Oldstone, M.B., and Lemke, G. 2007. TAM receptors are pleiotropic inhibitors of the innate immune response. *Cell.* 131:1124-1136.
118. O'Neill, N.A.J. 2007. TAMpering with Toll-like receptor signaling. *Cell.* 131:1039-1041.
119. Seitz, H.M., Camenisch, T.D., Lemke, G., Earp, H.S., and Matsushima, G.K. 2007. Macrophages and dendritic cells use different Axl/Mertk/Tyro3 receptors in clearance of apoptotic cells. *J. Immunol.* 178:5635-5642.
120. Wallet, M.A., Sen, P., Flores, R.R., Wang, Y., and Yi, Z. 2008. MerTK is required for apoptotic cell-induced T cell tolerance. *J. Exp. Med.* 205:219-232.
121. Tibrewal, N., Wu, Y., D'Mello, V., Akakura, R., George, T. C., *et al*. 2008. Autophosphorylation docking site Tyr-867 in Mer receptor tyrosine kinase allows for dissociation of multiple signaling pathways for phagocytosis of apoptotic cells and down-modulation of lipopolysaccharide-inducible NF-kappaB transcriptional activation. *J. Biol. Chem.* 283:3618-3627.
122. Kushwah, R., and Hu, J. 2010. Dendritic cell apoptosis: regulation of tolerance versus immunity. *J. Immunol.* 185:795-802.
123. Chen M., W., Y.H., Wang, Y., Huang, L., Sandoval, H., *et al*. 2006. Dendritic cell apoptosis in the maintenance of immune tolerance. *Science.* 311:1160-1164.
124. Kushwah, R., Oliver, J.R., Zhang, J., Siminovitch, K.A., and Hu, J. 2009. Apoptotic dendritic cells induce tolerance in mice through suppression of dendritic cell maturation and induction of antigen-specific regulatory T cells. *J. Immunol.* 183:7104-7118.
125. Kushwah, R., Wu, J., Oliver, R., Jiang, G., Zhang, J, *et al*. 2010. Uptake of apoptotic DCs converts immature DC into tolerogenic DC that induce differentiation of Foxp3+ Tregs. *Eur. J. Immunol.* 40:1022-1035.
126. Huynh M.L.N., F., V.A., and Henson, P.M. 2000. Phosphtidylserine-dependent ingestion of apoptotic cells promotes TGF-β1 secretion and the resolution of inflammation. *J. Clin. Invest.* 109:41-50.
127. Hoffmann, P.R., Kench, J.A., Vondracek, A., Kruk, E., Daleke, D.L., *et al*. 2005. Interaction between phosphatidylserine and the phosphatidylserine receptor inhibits immune responses in vivo. *J. Immunol.* 174:1393-1404.
128. Rivas, J., and Ullrich, S. 1992. Systemic suppression of delayed-type hypersensitivity by supernatants from UV-irradiated keratinocytes. An essential role for keratinocyte-derived IL-10. *J. Immunol.* 149:3865-2871.
129. Neuner, P., Charvat, B., Knobler, R., Kirnbauer, R., Schwarz, A., *et al*. 1994. Cytokine release by peripheral blood mononuclear cells is affected by 8-methoxypsoralen plus UV-A. *Photochem. Photobiol.* 59:182-188.

130. Morelli, A.E., Larregina, A.T., Shufesky, W.J., Zahorchak, A.F., and Logar, A.J. 2003. Internalization of circulating apoptotic cells by splenic marginal zone dendritic cells: dependence on complement receptors and effect on cytokine production. *Blood.* 101:611-620.
131. Crispe, I.N., Giannandrea, M., Klein, I., John, B., Sampson, B., and Wuensch, S. 2006. Cellular and molecular mechanisms of liver tolerance. *Immunol. Rev.* 213:101-118.
132. Huang, L., Soldevila, G., Leeker, M., Flavell, R., and Crispe, I.N. 1994. The liver eliminates T cells undergoing antigen-triggered apoptosis in vivo. *Immunity.* 1:741-749.
133. Fimiani, M., Rubegni, P., Pimpinelli, N., Mori, M., De Aloe, G., and Andreassi, L. 1997. Extracorporeal photochemotherapy induces a significant increase in CD36+ circulating monocytes in patients with mycosis fungoides. *Dermatology.* 194:107-110.
134. Divito, S.J., Wang, Z., Shufesky, W. J., Liu, Q., Tkacheva, O. A., *et al*. 2010. Endogenous dendritic cells mediate the effects of intravenously injected therapeutic immunosuppressive dendritic cells in transplantation. *Blood.* 116:2694-2705.
135. Girardi, M., Heald, P.W., and Wilson, L.D. 2004. The pathogenesis of mycosis fungoides. *N. Engl. J. Med.* 350:1978-1988.
136. Campbell, J.J., Clark, R.A., Watanabe, R., and Kupper, T.S. 2010. Sezary syndrome and mycosis fungoides arise from distinct T-cell subsets: a biologic rationale for their distinct clinical behaviors. *Blood.* 116:767-771.
137. Lin, W.M., Lewis, J.M., Filler R.B., Modi, B.G., Carlson, K.R., *et al.* 2012. Characterization of the DNA copy-number genome in the blood of cutaneous T-cell lymphoma patients. *J. Invest. Dermatol.* 132:188-197.
138. Akilov, O.E., Wu, M.X., Ustyugova, I.V., Falo L.D., and Geskin, L.J. 2012. Resistance of Sezary cells to TNF-alpha-induced apoptosis is mediated in part by a loss of TNFR1 and a high level of the IER3 expression. *Exp. Dermatol.* 21:287-292.
139. Wang, Y., Su, M., Zhou, L.L., Tu, P., Zhang, X., *et al*. 2011. Deficiency of SATB1 expression in Sezary cells causes apoptosis resistance by regulating FasL/CD95L transcription. *Blood.* 117:3826-3835.
140. Lamprecht, B., Kreher, S., Mobs, M., Sterry, W., Dorken, B., *et al*. 2012. The tumor suppressor p53 is frequently nonfunctional in Sezary syndrome. *Br. J. Dermatol.* 167:240-246.
141. McCusker, M.E., Garifallou, M., and Bogen, S.A. 1997. Sezary lineage cells can be induced to profilerate via CD28-mediated costimulation. *J. Immunol.* 158:4984-4991.
142. Gurung, P., Kucaba, T.A., Ferguson, T.A., and Griffith, T.S. 2009. Activation-induced CD154 expression abrogates tolerance induced by apoptotic cells. *J. Immunol.* 183:6114-6123.
143. Van der Fits, L., Out-Luiting, J.J., Van Leeuwen, M.A., Samsom, J.N., Willemze, R., *et al*. 2012. Autocrine IL-21 stimulation is involved in the maintenance of constitutive STAT3 activation in Sezary syndrome. *J. Invest. Dermatol.* 132:440-447.

144. Krzysiek, R. 2010. Role of glucocorticoid-induced leucine zipper (GILZ) expression by dendritic cells in tolerance induction. *Transplant. Proc.* 42:3331-3332.
145. Lebson, L., Wang, T., Jiang, Q., and Whartenby, K.A. 2011. Induction of the glucocorticoid-induced leucine zipper gene limits the efficacy of dendritic cell vaccines. *Cancer Gene Ther.* 18:563-570.